027595-F

A MILLIMETER-WAVE RADIOMETER TECHNIQUE FOR MEASURING ICE THICKNESS ON THE SURFACE OF THE SPACE SHUTTLE'S EXTERNAL FUEL TANK

Fawwaz T. Ulaby (PI)
John R. Kendra
Thomas F. Haddock
Steve Wu (NASA Stennis Space Center)

Final Technical Report
NASA Stennis Space Center Contract NAG13-12

February, 1991

engn

UMR 0407

Contents

List of Figures

List of Tables

Abstract

The external fueltank of the Space Shuttle contains extremely low-temperature propellents. A layer of material known as SOFI (Spray-On Foam Insulation), covering the outside of the fueltank provides thermal insulation between the aluminum surface of the fueltank and the ambient air. In spite of this insulation, under certain conditions ice formation will occur on the surface of the SOFI. Ice on the external fueltank can be detrimental to the launch and it is important to detect its presence and measure its thickness. This paper describes the design of a millimeter-wave radiometer technique developed for this purpose. The design is based on model calculations and measurements— performed at 35, 94 and 140 GHz—of the emission properties of a panel from the external fueltank. We present experimental evidence demonstrating that the model can predict with a very reasonable degree of accuracy the emission from an ice/SOFI system for which the normally rough surface of the SOFI had been sanded smooth. We further show how this technique, performed on an isothermal system, can be extended to the more realistic case of a system in which a temperature gradient exists. For the case of the original, rough-surface SOFI covered with an ice layer, the observed emission is considerably modified from what is predicted by the model.

1 Introduction

The objective of this study is to investigate the feasibility of using a millimeter-wave imaging radiometer to detect the presence and measure the thickness of ice when it forms on the surface of the external fuel tank of the Space Shuttle. A conceptual design is shown in Figure 1. The radiometer antenna consists of a cylindrical reflector fed by a monolithic array of mixer elements. The array will produce continuous beams on the fuel tank surface. By rotating the array about its own axis, the surface will be imaged in the vertical dimension, thereby producing a two-dimensional image of the surface.

For any given beam, the antenna temperature of the fuel tank surface is given by [1]:

$$T_A = T_B + R\,T_{SKY}, \tag{1}$$

where T_B is the brightness temperature of the fuel tank surface, R is its reflectivity, and T_{SKY} is the incident sky radiation. In the conceptual design shown in Figure 1, after the feed array completes its scan of the antenna reflector (as it rotates about its own axis), it will observe the sky radiation directly through a focusing lens. The observation direction will be the same as that of the sky radiation incident upon the fuel tank surface. Hence, T_{SKY} will be measured directly.

The presence of ice on the fuel tank will affect T_A, through both T_B and R. However, T_A also depends on T_{SKY} and is related to the physical temperature of the medium through T_B. What is needed is a parameter that can be measured and unambiguously related to the ice thickness.

For the special case of an isothermal system with a specular surface, the emissivity e and reflectivity R are related by

$$R = 1 - e. \tag{2}$$

Upon using (2) in (1), and replacing T_B with eT_{PHYS}, where T_{PHYS} is the physical temperature of the medium, and then solving for e, we obtain:

$$e = \frac{T_A - T_{SKY}}{T_{PHYS} - T_{SKY}}\ , \tag{3}$$

The emissivity is related to only the electromagnetic properties of the system and will be the same for a given ice thickness regardless of the particular values of T_{SKY} or T_{PHYS}.

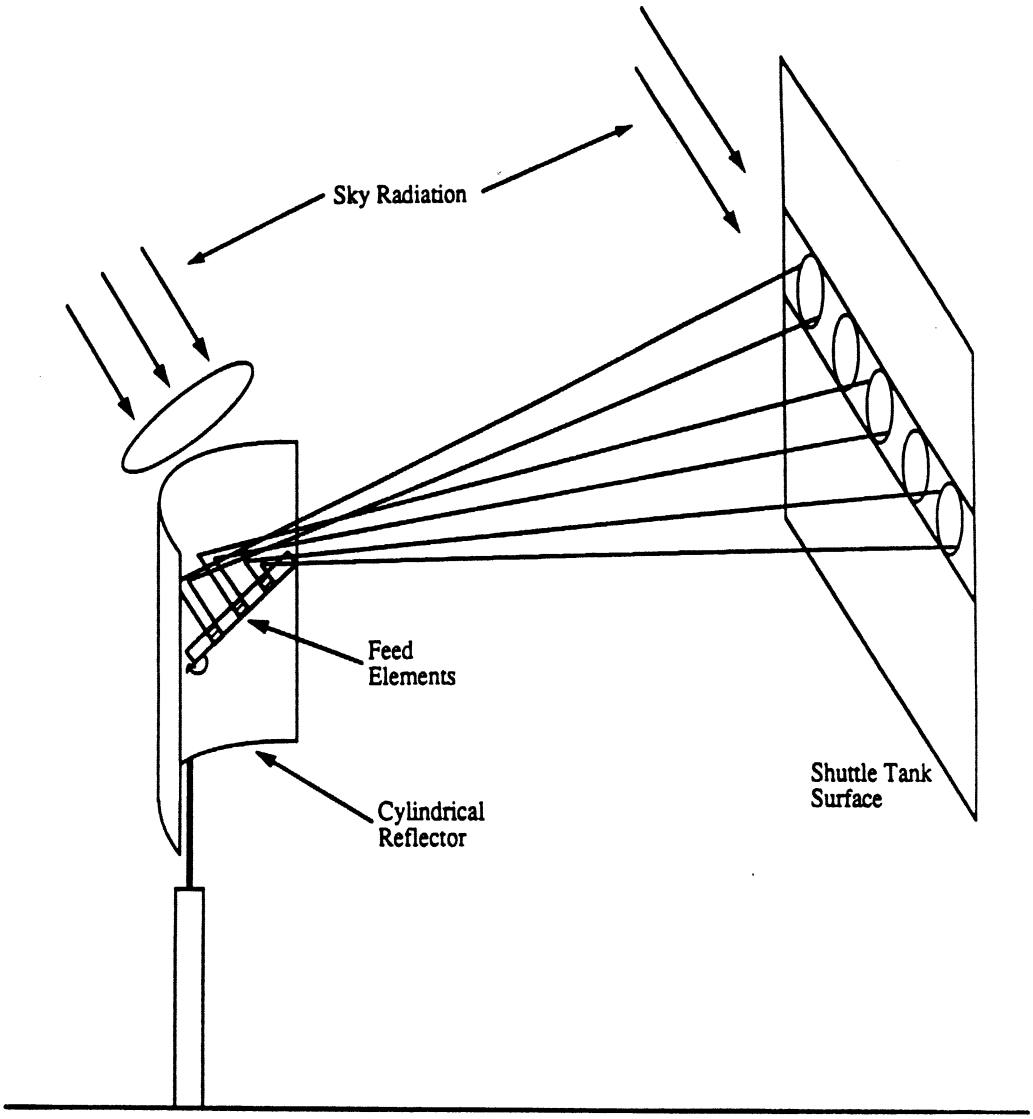

Figure 1: A conceptual configuration for an imaging millimeter-wave radiometer that uses a linear antenna array to feed a cylindrical reflector. As the array rotates about its own axis, the beams scan the shuttle tank surface along the vertical direction. At its end position, the array views the sky radiation through a focusing lens.

In our investigation, we will determine how emissivity can be related to ice thickness, thereby providing a means to measure the latter, in the isothermal case. Finally, we will demonstrate how this same procedure can be applied to the case of a temperature gradient, which more closely resembles the actual situation with the fuel tank. For this case, where (2) is no longer completely valid, we introduce the concept of an *effective emissivity*, e_{eff}.

2 Characterization of SOFI Material

In order to model the emissivity of the system consisting of an ice layer over the fuel tank surface, it is necessary to know certain electromagnetic properties of each of the components that comprise the system. In this section, we analyze the emissive characteristics of the fuel tank surface by itself, without ice.

The wall of the fuel tank consists of metal covered by a layer of foam material known as SOFI (**S**pray-**O**n **F**oam **I**nsulation), having a thickness of approximately 3.9 centimeters. According to Wu [2], the temperature at the metal-SOFI interface (Figure 2) is on the order of 94 K (or $-179°$ C) and the temperature in the ice layer is a few degrees below the freezing temperature of water; i.e., typically 270K (or $-3°$ C). The first step of this investigation is to determine whether this material behaves (electromagnetically) like a homogeneous layer or an inhomogeneous layer. If the material is homogeneous in behavior, coherent emission models are applicable, whereas if it is inhomogeneous, incoherent emission models should be used instead. The appropriate model can then be used in determining the relative dielectric constant of the SOFI material. The behavior of this fuel tank wall material is examined with respect to emissivity as a function of incidence angle. Figure 3 shows the arrangements used to measure T_{SKY} and T_A, from which $e(\theta)$ is computed according to (3). For each angle θ (Figure 3), T_{SKY} was measured by observing a flat metal panel, and then T_A was measured after replacing the metal panel with the SOFI panel. The measurements were conducted at 35, 94, and 140 GHz, for both horizontal and vertical polarizations. All three radiometers used 15-cm diameter corrugated-lens horn antennas with beamwidths of 3.2° at 35 GHz,1.4° at 94 GHz, and 0.9° at 140 GHz. Radiometer calibration was achieved by placing each of two specially

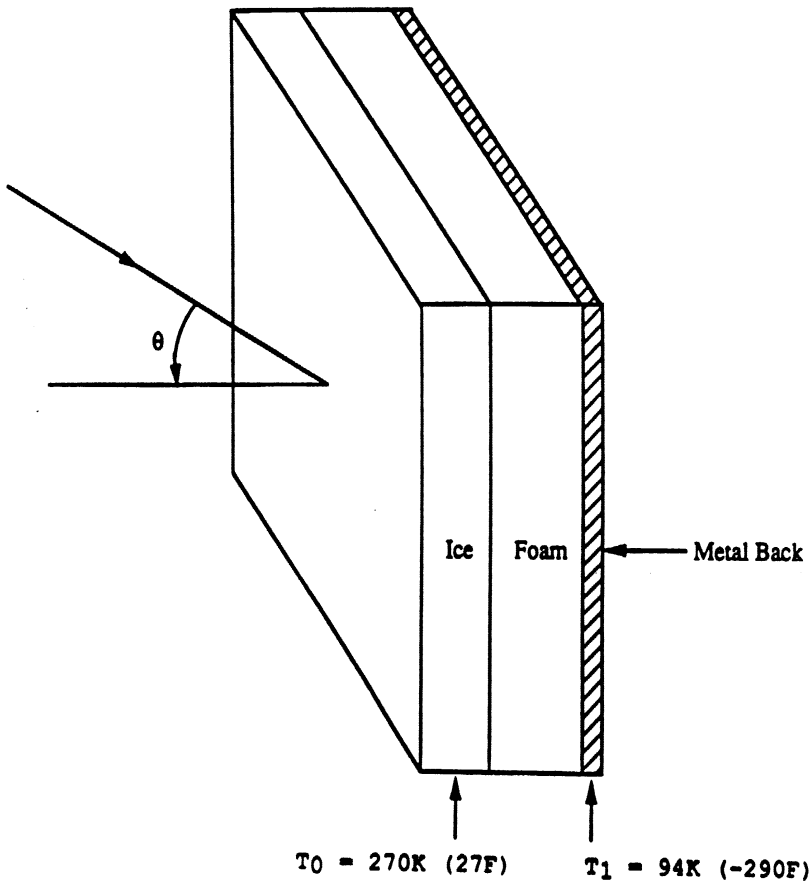

Figure 2: The tank surface is covered with a foam layer, approximately 3.9 cm thick, on the surface of which ice can form by condensation and freezing. The foam layer, called SOFI (**S**pray **O**n **F**oam **I**nsulation), acts as a thermal insulator between the low temperature metal surface and the outside environment.

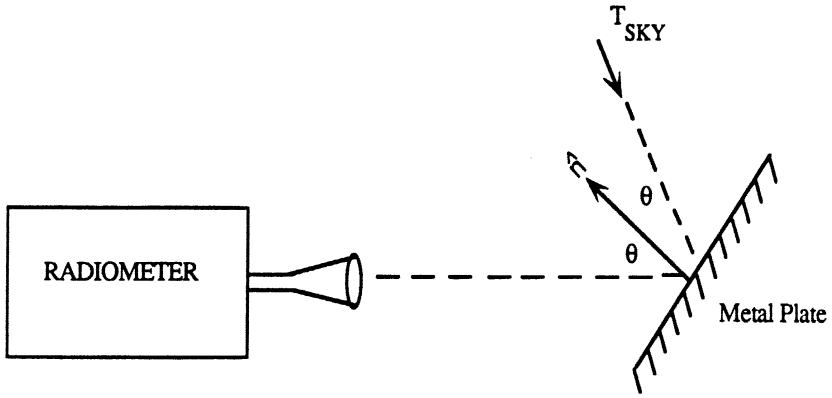

(a) Measurement of T_{SKY}.

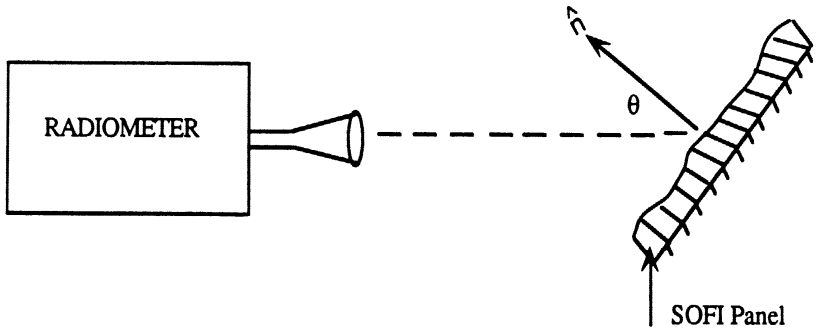

(b) Measurement of emission by SOFI Panel.

Figure 3: The arrangements used for measuring (a) T_{SKY} and (b) the antenna temperature due to emission by the SOFI panel. The angle θ can be adjusted to cover the range from 20° to 70°.

constructed panels of absorbing material (with emissivity $\simeq 1$) immediately in front of the antenna and then measuring the output voltage. The first panel is at the ambient air temperature and the second panel is at a temperature of 77K, achieved by pouring liquid nitrogen into the absorbing material through narrow holes cut into the material. The physical temperatures are measured by thermistors imbedded inside the material.

As noted earlier, the relationship of (2) is exact if the surface of the material is perfectly flat and if isothermal conditions exist. In our case, the SOFI panel has a rough surface. To evaluate the effect of the rough surface on the validity of (2), two sets of measurements will be conducted. One set of measurements will examine the original, rough-surface SOFI panel, and the other will examine the SOFI panel after its surface had been sanded smooth.

The results of the measurements of the original (rough) SOFI panel are shown in Figures 4 - 6. These figures show the measured angular response of the emissivity e for 35, 94, and 140 GHz, respectively. We observe that except for small oscillations, the emissivity increases monotonically with increasing incidence angle all three frequencies for both polarizations.

The results from the smooth SOFI panel are shown in Figure 7. Except for an overall reduction in emissivity, due to the thickness of the layer having been reduced by the sanding process to 2.7 cm, the data resembles that of the rough panel.

Both test panels consist of a low-loss dielectric slab placed over a metal plate. For a homogeneous slab with plane boundaries, theory suggests that we should observe large oscillations as a function of incidence angle. The absence of such oscillations in the observed data is indicative that phase coherence of the multiple reflections between the lower and upper boundaries of the dielectric slab is not preserved, which can be attributed to lack of dielectric homogeneity of the slab material at the scale of the wavelength under consideration and/or to the roughness of the upper boundary. When the rough upper boundary is removed, as in the case of the smooth panel, the essential emission characteristics of the panel are unchanged. Evidently, the rough surface is not an important factor in the emission of the SOFI panel itself. From these results on both test panels, is clear that the emission by the SOFI panel should be modeled using an incoherent radiative transfer approach.

For an inhomogeneous slab of thickness d and a relative dielectric constant $\epsilon = \epsilon' - j\epsilon''$ supported by a metal back surface, radiative transfer theory

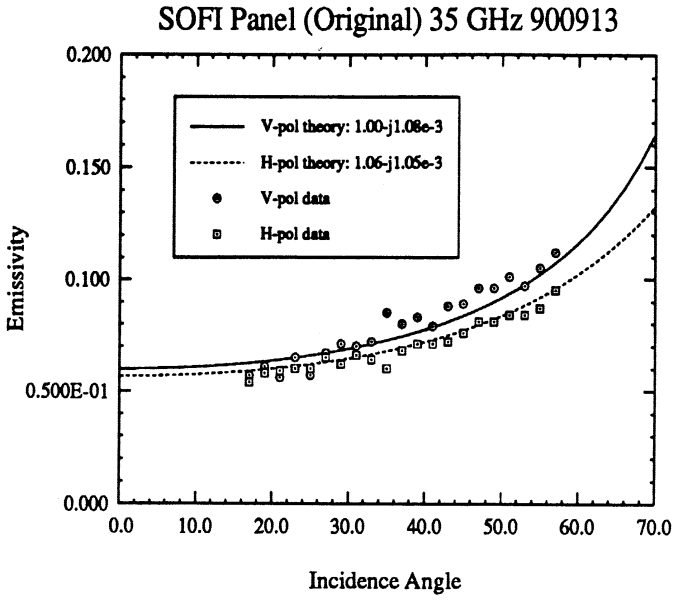

Figure 4: Measured and calculated emissivity of original rough-surface SOFI at 35 GHz.

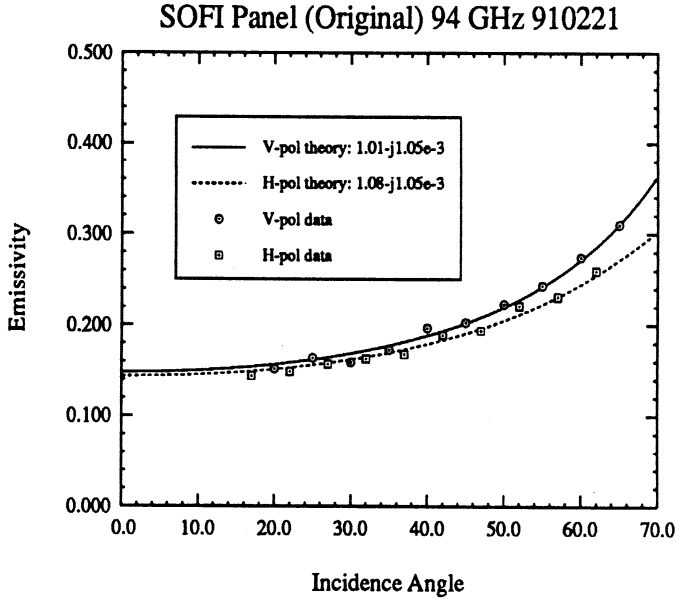

Figure 5: Measured and calculated emissivity of original rough-surface SOFI at 94 GHz.

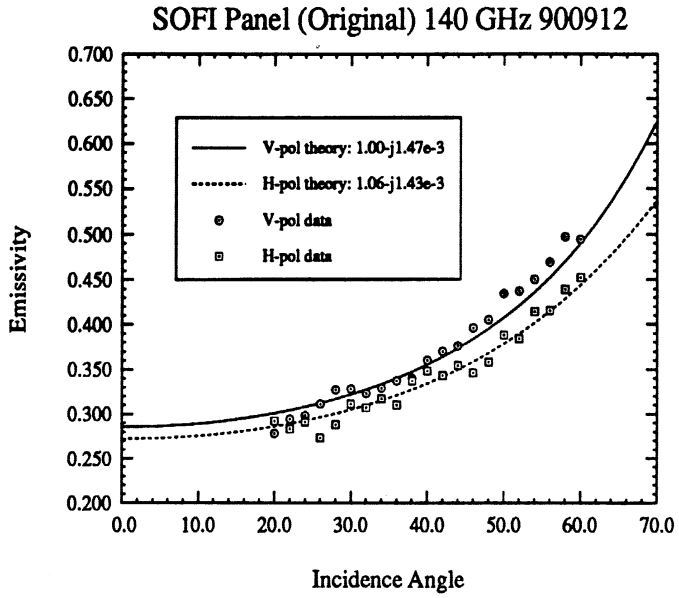

Figure 6: Measured and calculated emissivity of original rough-surface SOFI at 140 GHz.

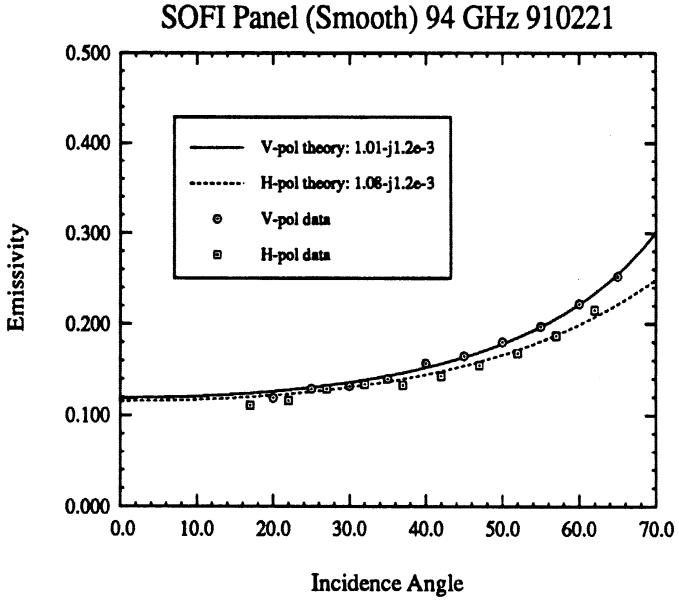

Figure 7: Measured and calculated emissivity of smooth-surface SOFI at 94 GHz.

provides the following expression for the emissivity $e_p(\theta)$ at incidence angle θ and antenna polarization p (v or h),

$$e_p(\theta) = \frac{(1 - \Upsilon^2(\theta))(1 - R(p,\theta))}{1 - \Upsilon^2(\theta)R(p,\theta)} \quad , \tag{4}$$

where

$$\begin{aligned} \Upsilon^2 &= \exp(-2\kappa\, d\, \sec\, \theta'), \\ \kappa &= \text{absorption coefficient of SOFI material}, \\ \theta' &= \sin^{-1}(\sin\theta/\sqrt{\epsilon'}) = \text{refraction angle}, \\ R(p,\theta) &= \text{Fresnel reflectivity of upper surface.} \end{aligned}$$

The Fresnel reflectivities $R(v,\theta)$ and $R(h,\theta)$ are given by

$$R(v,\theta) = \left| \frac{\epsilon\cos\theta - \sqrt{\epsilon - \sin^2\theta}}{\epsilon\cos\theta + \sqrt{\epsilon - \sin^2\theta}} \right|^2 , \tag{5}$$

$$R(h,\theta) = \left| \frac{\cos\theta - \sqrt{\epsilon - \sin^2\theta}}{\cos\theta + \sqrt{\epsilon - \sin^2\theta}} \right|^2 , \tag{6}$$

and for a low-loss material, κ is given by the approximate expression:

$$\kappa \simeq \frac{2\pi}{\lambda}\frac{\epsilon''}{\sqrt{\epsilon'}}. \tag{7}$$

Using a 5-GHz dielectric probe, it was determined that ϵ' of the SOFI material is less than 1.3. For a material with such a relative permittivity, the Fresnel reflectivity at normal incidence is 0.004. This means that the emissivity, as given by (2), is approximately

$$e(\theta = 0) \simeq\ 1 - \Upsilon^2(0). \tag{8}$$

By extrapolating the measured data down to 0°, we obtain essentially (to within experimental error) the same value for v and h polarizations, as expected:

$$\begin{aligned} e(\theta = 0) &= 0.059 \text{ @ } 35 \text{ GHz (rough surface)} \\ e(\theta = 0) &= 0.145 \text{ @ } 94 \text{ GHz (rough surface)} \\ e(\theta = 0) &= 0.118 \text{ @ } 94 \text{ GHz (smooth surface)} \\ e(\theta = 0) &= 0.272 \text{ @ } 140 \text{ GHz (rough surface)} \end{aligned}$$

Upon using these values in (8), we obtain a value for Υ^2 (0) at each of the three frequencies. This, in turn, specifies the value of the ratio $\epsilon''/\sqrt{\epsilon'}$ from (7) at each frequency. Finally, with ϵ' treated as a free variable, (4) is used to compute $e_p(\theta)$ versus θ to determine the effective value of ϵ' that provides a good fit to the observed data. The result of this process is shown in Figures 4 - 7 where we observe that the calculated curves are in very good agreement with the data. The values of ϵ used in the calculations are, for the rough panel:

$$\begin{aligned} &\epsilon = 1.00 - j\ 1.08 \text{ x } 10^{-3} \text{ @ } 35 \text{ GHz for } v \text{ polarization} \\ &\epsilon = 1.06 - j\ 1.05 \text{ x } 10^{-3} \text{ @ } 35 \text{ GHz for } h \text{ polarization} \\ &\epsilon = 1.01 - j\ 1.05 \text{ x } 10^{-3} \text{ @ } 94 \text{ GHz for } v \text{ polarization} \\ &\epsilon = 1.08 - j\ 1.05 \text{ x } 10^{-3} \text{ @ } 94 \text{ GHz for } h \text{ polarization} \\ &\epsilon = 1.00 - j\ 1.47 \text{ x } 10^{-3} \text{ @ } 140 \text{ GHz for } v \text{ polarization} \\ &\epsilon = 1.06 - j\ 1.43 \text{ x } 10^{-3} \text{ @ } 140 \text{ GHz for } h \text{ polarization.} \end{aligned} \tag{9}$$

For the smooth panel, the values of ϵ are:

$$\begin{aligned} &\epsilon = 1.00 - j\ 1.20 \text{ x } 10^{-3} \text{ @ } 94 \text{ GHz for } v \text{ polarization} \\ &\epsilon = 1.06 - j\ 1.20 \text{ x } 10^{-3} \text{ @ } 94 \text{ GHz for } h \text{ polarization.} \end{aligned} \tag{10}$$

These results raise two questions: (a) why is ϵ slightly different for the two polarizations, and (b) why is the value of ϵ for the smooth-surface panel slightly different from that of the rough-surface panel? The answers to both of these questions lies in the structure of the SOFI material. It is not actually a continuous slab, but has instead four or five layers of identical material,

separated by thin darker layers. These layers are evidently produced in the application process, with the darker layers appearing where the surface of the SOFI layer had dried exposed to the air.

We examined the emission behavior of such structures—low dielectric, multi-layered, and backed by a metal plate—using computer simulations. These simulations revealed that the observed divergence between the two polarizations is indeed consistant with the theoretical behavior of such a structure. An additional effect revealed by the simulations is that the magnitude of the emissivity of such a layered structure tends to be much lower than that of a corresponding continuous slab having the same dielectric constant.

In light of the above discussion, we can make the following inferences regarding our experimentally derived values of ϵ:

- The values of ϵ we have found are *effective* values (particularly for ϵ''). The actual value of ϵ'' for the SOFI material is likely higher but is reduced by the layering.

- The fact that the value of ϵ'' for the *smooth* panel is higher than that of the rough panel is consistant with the previous remark. In smoothing the surface we removed approximately 1 cm of the slab, thereby reducing the number of layers. Less layering translates into higher emissivity and therefore a greater perceived value for ϵ''.

For the purposes of this study, the true value of ϵ for the SOFI panel is unimportant. It is sufficient that the emission characteristics are consistant with our description of the material as a continuous slab having dielectric constants given in (9) and (10). These values of ϵ will be used in succeeding sections to calculate the emission behavior of the SOFI panel when covered by a sheet of ice.

3 Determination of Ice Dielectric Properties

As discussed earlier, under certain conditions, the presence of a cold SOFI panel surface induces the formation of ice (or frost) through condensation and freezing of water vapor from the ambient environment. This frost layer is likely to be a combination of air and ice particles, which raises two questions:

(a) what is an appropriate value of the ice volume fraction that should be used in characterizing the dielectric of the frost layer, and (b) what is the dielectric constant of ice at the frequencies under consideration in this study?

3.1 Ice Volume Fraction

Due to the lack of information pertinent to the first question, we should keep the ice volume fraction as an unknown variable for the present. However the form of the computations which will be associated with this parameter are as detailed below.

To compute the dielectric constant of a frost layer, ϵ_1, we shall assume that the ice particles in the layer are spherical in shape and much smaller than λ in size, in which case we can use the mixing model [1, Appendix E]

$$\epsilon_1' = \frac{1 + 0.835\ v}{1 - 0.417\ v}, \tag{11}$$

$$\epsilon_1'' = \frac{0.34\ v\ \epsilon_i''}{(1 - 0.417\ v)^2}, \tag{12}$$

where v is the ice volume function. In emission calculations presented later in this report, we shall consider two cases for v, namely $v = 0.5$, which we shall refer to as frost, and $v = 1$ representing pure ice.

3.2 Ice Dielectric Properties

3.2.1 Theory

For pure ice, the relative dielectric constant ϵ_i is given by

$$\epsilon_i = \epsilon_i' - j\epsilon_i'', \tag{13}$$

with $\epsilon_i' = 3.15$, independent of temperature and frequency at microwave and millimeter-wave frequencies [1, Appendix E]. The imaginary part, ϵ_i'', on the other hand, exhibits a strong dependance on frequency and a weak dependence on temperature [1].

To determine the dielectric constant of the ice used in this study we used the same technique employed by Mätzler and Wegmüller [3] in an extensive ice study undertaken in 1987. The procedure involves observing, at the

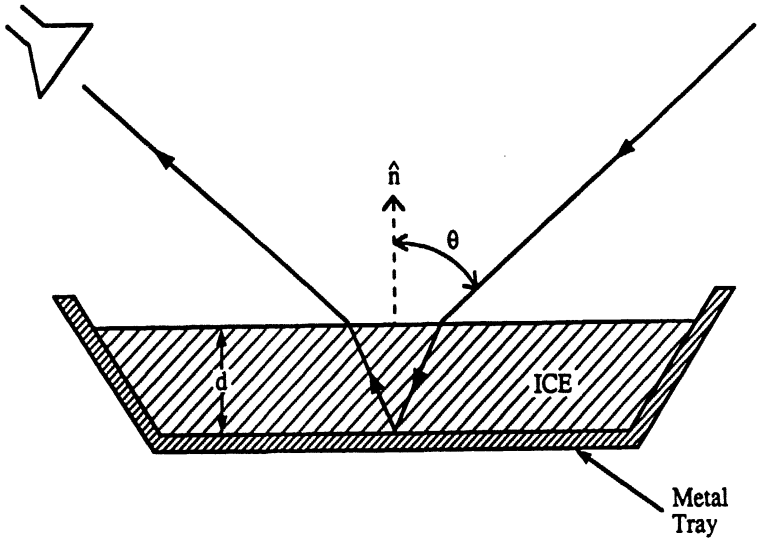

Figure 8: Schematic of experimental setup used to measure the radiometric temperature of ice. The results of such experiments were used to calculate the dielectic constant of ice.

Brewster angle, θ_B, the vertically polarized emission from a layer of ice over a metal surface. The setup is illustrated in Figure 8. The sky brightness, T_{SKY}, suffers no reflection at the air/ice interface, either entering or exiting the ice layer. Therefore, the effective reflectivity is just the amount by which T_{SKY} is attenuated by the ice layer. Thus,

$$R(\theta_B) = 1 - e(\theta_B) = \Upsilon^2(\theta_B), \tag{14}$$

where Υ^2 is as given in (4) and κ (contained in Υ) is as given in (7). Since ϵ_i' is known, ϵ_i'' can be calculated directly.

In addition to observing the ice at the Brewster angle, as an additional check, we further measured the emissivity at other incidence angles between 15° and 70°. This was done using the same technique described for the SOFI panel. If the value for ϵ_i'' calculated from the Brewster angle is correct, then

the emissivities measured at other incidence angles should be predicted by an emission model utilizing ϵ_i''.

As previously mentioned, two cases are possible: a coherent model and an incoherent radiative transfer model. The latter is given in equation (4). The coherent model of a slab of dielectric material over a metal plate is given by the following expression [4]:

$$e_c(p,\theta) = 1 - R_c(p,\theta)$$

with

$$R_c = \left(\frac{R(p,\theta) + \Upsilon^2(\theta) + 2\sqrt{R(p,\theta)}\Upsilon(\theta)\cos(2\beta' d + \phi - \pi)}{1 + \Upsilon^2(\theta)R(p,\theta) + 2\sqrt{R(p,\theta)}\Upsilon(\theta)\cos(2\beta' d - \phi - \pi)} \right), \qquad (15)$$

where

$$\beta' = \frac{2\pi}{\lambda}\cos\theta',$$

d is the slab thickness, $R(p,\theta) = |r(p,\theta)|^2$ is the Fresnel reflectivity of the air-ice interface and ϕ is the phase angle of $r(p,\theta)$.

3.2.2 Results

At 35 GHz the measurement process was performed at both polarizations for an ice layer whose thickness was measured to be 7.5 $\pm$ 1 mm. As shown in Figure 9, the data is in good agreement with calculations based on coherent model. This model uses $\epsilon_i'' = 5.6 \times 10^{-3}$, the value obtained by evaluation of e_c near the Brewster angle. Some small adjustment of the ice thickness parameter d was required to achieve an acceptable fit. Another series of measurements was made at 35 GHz for a thicker ice layer, 10 $\pm$ 1 mm. Although the value of emissivity measured at the Brewster angle is consistent with the value of ϵ_i'' obtained above for the lesser thickness, neither model provides an acceptable fit to the measured data at *other* incidence angles. It is possible that at this thickness the source of the emission is from a combination of coherent and incoherent processes. Note that the Brewster angle is the only angle at which both the coherent and incoherent models will always give the same result; this is a consequence of the reflectivity at the air/ice interface being zero — no multiple internal reflections are possible. It is therefore significant that, regardless of what emissivities are measured

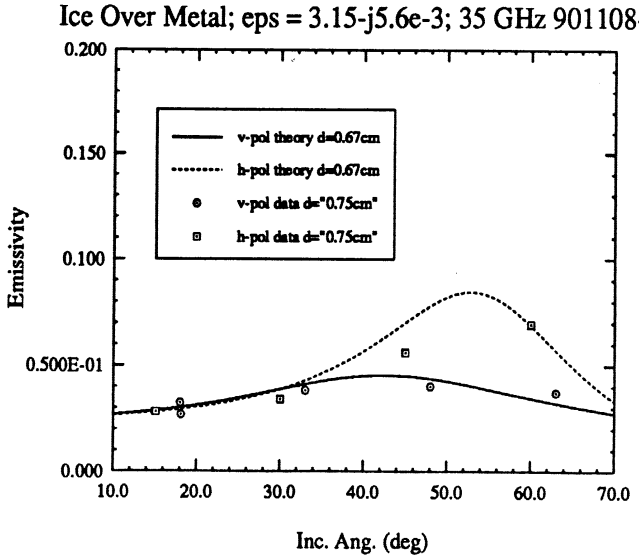

Figure 9: Experimental results of ice layer measurements at 35 GHz. Curves fitted to data were generated using a coherent-emission model with $\epsilon_{ICE} = 3.15 - j5.6 \text{ x } 10^{-3}$.

at other incidence angles, the emissivity measured at the Brewster angle is consistant with the first result.

At 94 GHz we again observed two different thicknesses of ice, but this time using only vertical polarization. As shown in Figure 10, a very good fit was achieved using the incoherent model. For both cases, ϵ_i'' was found to be 1.14 x 10^{-2}. As in the case of 35 GHz, some slight adjustment of the thickness d was required to achieve this agreement.

In the aforementioned study perfomed by Mätzler and Wegmüller, their measurements of ϵ_i'' cover several frequencies extending from 2.4 GHz to 94 GHz, for both pure and impure ice. Table 1 provides a comparison of their data for impure ice with our experimentally determined values of ϵ_i''. The two sets of measurements are in close agreement, particularly at 94 GHz.

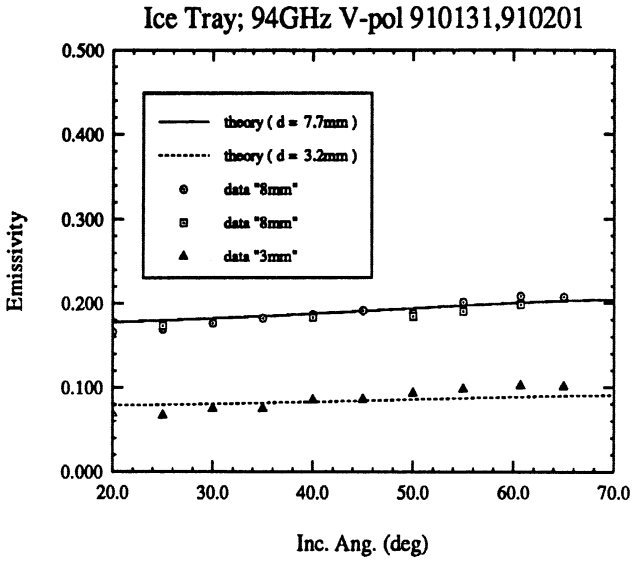

Figure 10: Experimental results of ice layer measurements at 94 GHz. for V-polarization. Curves fitted to data were generated using an incoherent-emission model with $\epsilon_{ICE} = 3.15 - j1.14 \text{ x } 10^{-2}$.

Freq. (GHz)	Previously Reported*	This Study
35	$4.6 \text{ x } 10^{-3}$	$5.6 \text{ x } 10^{-3}$
94	$1.13 \text{ x } 10^{-2}$	$1.14 \text{ x } 10^{-2}$

*Mätzler and Wegmüller, 1987.

Table 1: Experimentally determined values of ϵ_i'' for impure ice.

4 Emission Model For Ice Layer Over SOFI Panel

4.1 Smooth-Surface SOFI Panel

The values obtained for the dielectric constant of the SOFI panel and of the ice are the critical parameters in the final model which will predict emissivity as a function of ice thickness on the SOFI panel. Additionally, except possibly for thin ice layers examined at 35 GHz, we have shown that the materials separately exhibit emission characteristics corresponding to incoherent processes. Since our measurements will principally involve the 94 GHz channel, it is therefore appropriate to use incoherent radiative transfer theory to model the emission of the ice-SOFI structure. Appendices A and B provide expressions for the brightness temperature T_B of an ice (or frost) layer of dielectric constant ϵ_1 and thickness d_1 over a SOFI layer of dieletric constant ϵ_2 and thickness $d_s = d_2 - d_1$. The first appendix considers the uniform temperature case with $T(z) = T_0$ in both layers (illustrated in Figure 11), and the second appendix considers the case where $T(z)$ varies linearly from T_1 at the backside of the SOFI panel to T_0 at the SOFI-ice boundary (Figure 12). The final expression for the emission from the uniform temperature, or isothermal, case is given by:

$$e = (1 - R_0)\left[\frac{(1 - R_1\Upsilon_2^2) - R_1\Upsilon_1^2(1 - \Upsilon_2^2) - \Upsilon_1^2\Upsilon_2^2(1 - R_1)}{(1 - R_1\Upsilon_2^2)(1 - R_0R_1\Upsilon_1^2) - \Upsilon_1^2\Upsilon_2^2R_0(1 - R_1)^2}\right]T_0, \quad (16)$$

where

$$\begin{aligned}
\Upsilon_1 &= \exp(-\kappa_1 d_1 \sec\theta_1), \\
\Upsilon_2 &= \exp[-\kappa_2(d_2 - d_1)\sec\theta_2], \\
\kappa_1 &= \frac{2\pi}{\lambda}\frac{\epsilon_1''}{\sqrt{\epsilon_1'}}, \\
\kappa_2 &= \frac{2\pi}{\lambda}\frac{\epsilon_2''}{\sqrt{\epsilon_2'}}, \\
\theta_1 &= \sin^{-1}\left(\sin\theta_o/\sqrt{\epsilon_1'}\right),
\end{aligned}$$

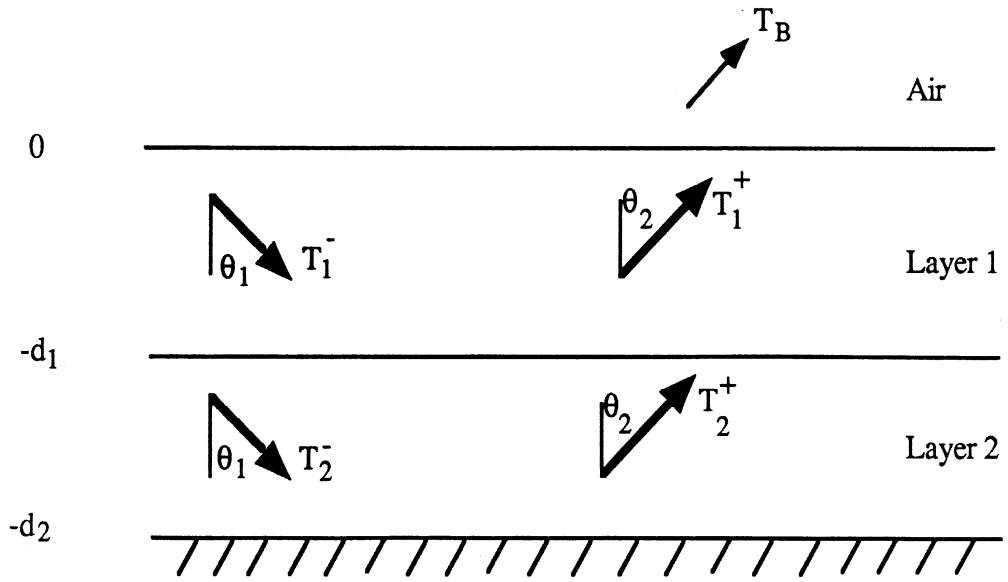

Figure 11: Geometry of emission for uniform temperature profile case. The quantities T_1^+ and T_2^+ represent upwelling radiation in layers 1 and 2, and T_1^- and T_2^- represent downwelling radiation.

$$\theta_2 = \sin^{-1}\left(\sin\theta_o/\sqrt{\epsilon_2'}\right),$$

and where R_0 and R_1 are the Fresnel reflectivities of the air/ice and ice/SOFI interfaces, respectively, for which expressions are given in (A.13) and (A.14) in Appendix A.

4.2 Rough-Surface SOFI Panel

Experimental results (given later) indicate that the rough surface of the SOFI panel significantly modifies the emission from the ice-SOFI structure. The rough surface was unimportant when observations were made of the SOFI panel alone because of the very small dielectric contrast between the SOFI and air. When ice-covered however, it becomes a rough interface of significant dielectric contrast. No model is proposed at present for the emission from this structure. This will be the subject of future work.

The expression given by (16) will be used in Sections 6 and 7 to compare model calculations with measured data. Emission by the ice-over-SOFI panel in the non-isothermal case is characterized by the brightness temperature

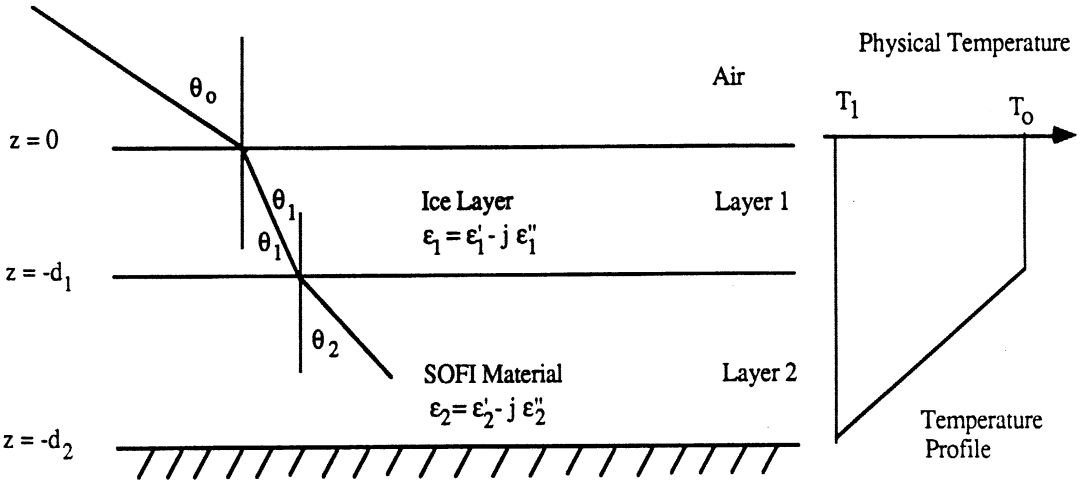

Figure 12: Geometry of emission for linear temperature profile in layer 2, $T(z) = T_0 + (z + d_1)(T_0 - T_1)/(d_2 - d_1)$for $-d_2 \leq z \leq -d_1$ and a uniform profile in layer 1, $T(z) = T_0$for $-d_1 \leq z \leq 0$.

expression given in Appendix B, which will be used in Section 7.2 to examine the dependence on ice thickness.

5 Experimental Considerations

5.1 General Setup

The experimental measurements were performed using a three-channel linearly-polarized radiometer with operating frequencies at 35, 94, and 140 GHz. In order to incorporate the unobstructed sky irradiance, the experiments were performed on the roof of one of the University's buildings. The setup of a typical experiment was as shown in Figure 13a. A frame constructed around the radiometer allowed the polarization to be selected by rotating the entire radiometer system to achieve the desired polarization. Two mounts were constructed. The first was designed to cradle the radiometer, and allowed positioning between the angles of 0° (pointing straight down) and 180° (straight up). The other mount, identical in design, supported a metal-backed tray into which various targets could be placed for observation, and which was

positionable for incidence angles from 20° to 70°. Figure 13b shows a closer view of the target mount holding one of the ice-covered SOFI panels. The two mounts, for radiometer and target respectively, were then placed facing each other (Figure 13a) and separated by a distance corresponding to the far-field distance for the frequency of interest. For an aperture with diameter D, the far-field distance was computed according to the formula

$$Z \geq D^2/\lambda,$$

which corresponds to a maximum phase error of 45° across the aperture. For the three frequencies used, these distances were:

2.7 m	@	35 GHz
7.3 m	@	94 GHz
10.9 m	@	140 GHz

At these far-field distances, the footprint of the antenna beam was on the order of 15 cm in diameter.

The 1 KHz (frequency of Dicke switching) modulated output of the radiometers was fed into a lock-in amplifier (Stanford Instruments, model #SR510), and the resulting voltage was sampled by an IBM-compatible computer. The computer was programmed for amplifier control, data aquistion and storage, and computation and output of brightness temperature. A single sample represented the average of four voltage samples, each corresponding to an integration time of one second. The BASIC program, "Radcal6," is included in Appendix C.

A two point calibration procedure was performed, as described in Section 2 of this report, using liquid-nitrogen and ambient-temperature loads, both having emissivities of one. Accurate pointing of the radiometer was insured by rifle scopes mounted alongside each radiometer and antenna.

5.2 Target Preparation

Formation of the ice layer on the SOFI panel was achieved by using a freezer room that was maintained at a constant temperature of -20° C. The ice forming process consisted of applying a finely atomized spray of water to the SOFI panel in the cold room. By applying the water in this fashion successive thin coatings of ice were created, thereby minimizing the formation of bubbles

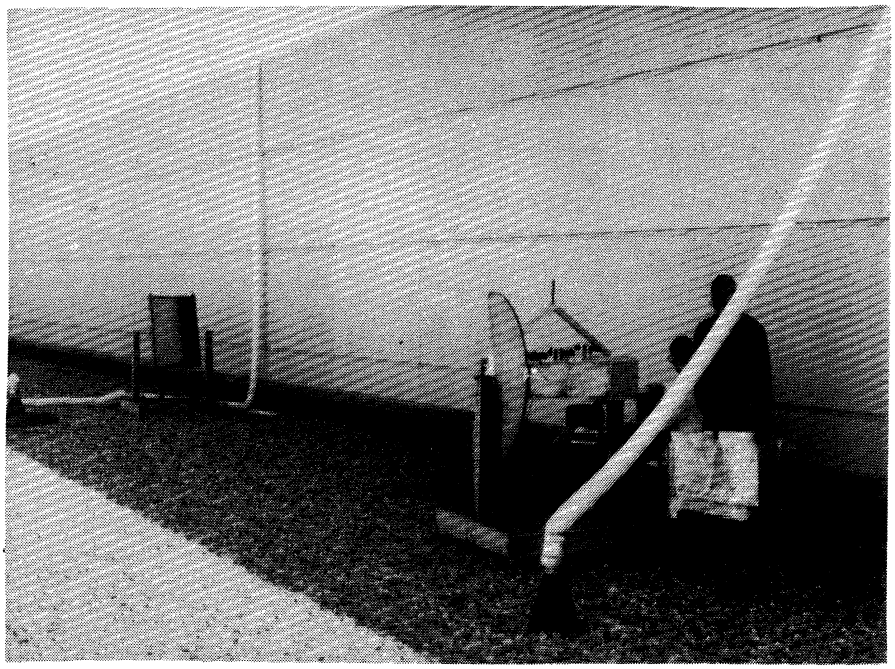

(a)

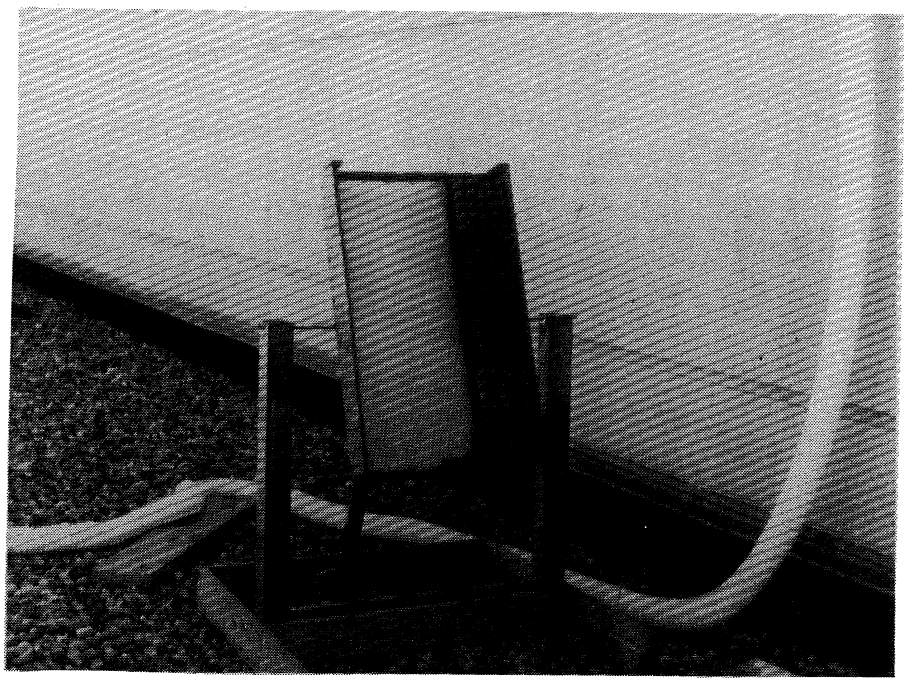

(b)

Figure 13: Photographs showing (a) experimental setup on roof, and (b) close-up of target mount holding SOFI panel with ice layer.

in the ice layer. Thin graduated posts stuck into the SOFI panel allowed the thickness of the ice layer to be determined with a precision better than ± 1 millimeter.

Once the ice had been formed, the panel was wrapped in an insulating pocket and quickly taken to the roof for observation. Several quick measurements were made and then the panel was returned to the freezer. It was important to conduct our measurements quickly not only to avoid having the ice melt, but also to prevent the warming of the panel which would invalidate the isothermal assumption used in the emissivity calculations. The measurements were made as a function of incidence angle over a range from 20° to 65°. To confirm that the ice-covered SOFI panel remained thermally constant over the duration of an experiment, an additional measurement was made at the end of each experiment at the angle corresponding to the first measurement. Reproducibility implied that the state of the panel had not changed during the measurement process. In colder, sub-freezing weather, it was only necessary to allow the panel to come to equilibrium with the ambient temperature to achieve the isothermal state.

5.3 Background Correction

Although the radiometer antennas had narrow beamwidths and small footprints, it was decided to account for and then remove the contributions to the total power received by the antenna emanating from regions outside of the target area, thereby improving the measured accuracy. The target area was 1 m x 41 cm, and the mainlobe footprint was 15 cm in diameter. In spite of the fact that the panel was much larger than the mainlobe footprint, significant side-lobe contributions were received by the radiometer from the radiometrically warm surroundings. Accordingly, the measured temperature was given by:

$$T_{AP} = \eta T_{ML} + (1 - \eta) T_{SL}, \tag{17}$$

where,

T_{AP} = Apparent (measured) temperature,
η = "Mainlobe" efficiency,
T_{ML} = Apparent temperature of "mainlobe" contribution,
T_{SL} = Apparent temperature of non-"mainlobe" contribution.

where the term "mainlobe" denotes the entire target area. The quantitiy of interest is T_{ML}, which is the antenna temperature T_A of the target.

The "mainlobe" efficiencies η were determined for each frequency and polarization. This was accomplished by using two known targets, to solve for the two unknowns in (16), η and T_{SL}. The two targets used were (a) the sky at a particular incidence angle, and (b) an absorbing target having an emissivity of one and whose physical temperature was known. The sky temperature was first measured by pointing the radiometer straight up; then the radiometer was pointed horizontally at a metal-plate target that was positioned at an incidence angle of 45°. With reference to equation (17), the T_{ML} in this case was the T_{SKY} measured at 180° (looking straight up). For the case of the absorber target, T_{ML} was simply T_{phys}, the physical temperature of the absorber. The measurements of these two targets provided the two equations, in the form of (17), needed to solve for the two unknowns, η and T_{SL}. Subtracting one of these equations from the other gives

$$\eta = \frac{T_{A1} - T_{A2}}{T_{SKY} - T_{ABS}} , \tag{18}$$

where

T_{A1} = Apparent temperature of metal plate at 45° ,
T_{A2} = Apparent temperature of absorber ,
T_{SKY} = Apparent temperature of sky at 180°,
T_{ABS} = Physical temperature of absorber.

Having found η for all frequencies and polarizations, the value of T_{SL} could be determined at any time by measuring T_{AP} for the aforementioned absorber target. Then from (17)

$$T_{SL} = \frac{T_{AP} - \eta T_{ABS}}{1 - \eta}.$$

The values of η and T_{SL} determined using the above procedure were then used in (17) to obtain T_{ML} for any target of interest from a measurement of T_{AP}. Table 2 gives an example of the effectiveness of the background correction technique. The table shows three separate measurements of the sky temperature when observed directly by positioning the radiometer at 180° (straight up), and those obtained (with background correction) by pointing

Sky Direct (K)	Sky Reflected (K)	ΔK
23.3	with correction 23.6	0.3
23.5	with correction 21.9	1.6
22.7	with correction 22.7	0.0
23.8	without correction 32.9	9.1

Table 2: Effect of background correction on measurement of sky temperature.

the radiometer at a metal plate oriented at 45°. It is seen that the error, ΔK, is between 0 K and 1.6 K. Without background correction, the error is 9.1 K.

6 Results

6.1 Ice Over Smooth-Surface SOFI Panel

The model proposed in Section 4 indicates that the 140 GHz channel would be the most sensitive to small changes in ice thickness, thus providing the best resolution. Unfortunately, after obtaining only a small amount of data on the rough-surface SOFI panel (presented later), the 140 GHz channel suffered a serious hardware failure and was not useable for the remainder of this study. Consequently, all of our experimental observations on the smooth-surface SOFI panel were made using the 94 GHz channel. The results of these observations are shown in Figure 14. The experiment involved examining, using only vertical polarization, four separate thicknesses of ice over the SOFI panel: 2,4,6, and 8 mm. For each ice layer, the emissivity of the ice/SOFI system was measured at three different incidence angles.

The results of the experiment are presented along with the theoretical curves generated using the model given in Section 4. This model uses the experimentally determined dielectric constants for the SOFI panel and for the ice, given in Sections 2 and 3, respectively. The agreement between the model and the actual measurements is quite reasonable.

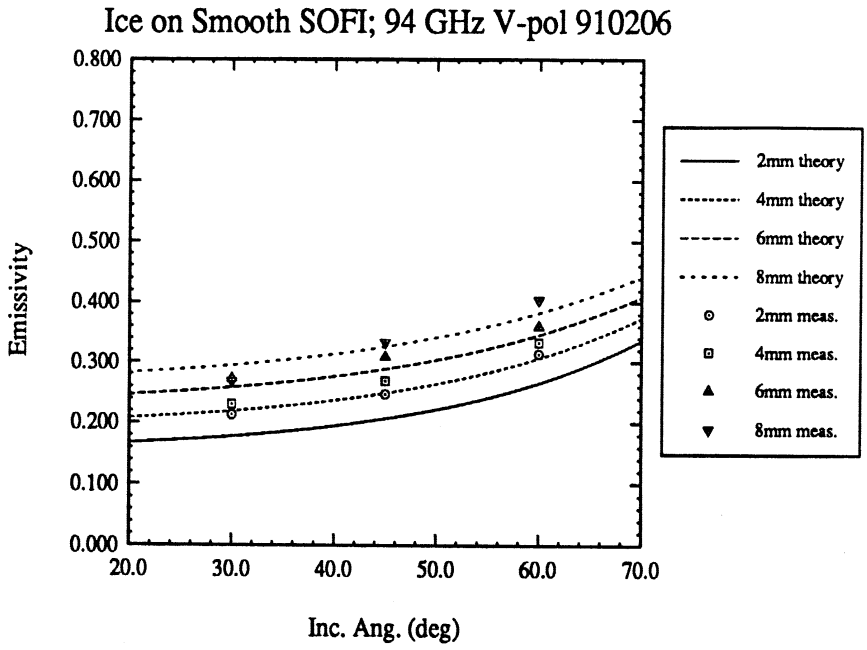

Figure 14: Measured and predicted emissivity, at 94 GHz, for *smooth-surface* SOFI panel for four different ice thicknesses.

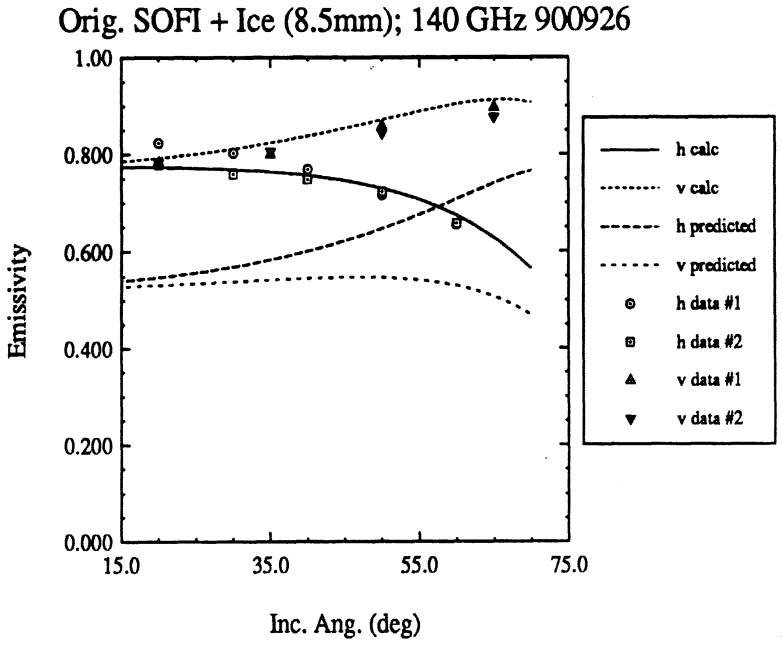

Figure 15: Experimental results obtained at 140 GHz for original rough-surface SOFI panel. The curves which were calculated to fit the data required using $\epsilon''_{ICE} = 5.2 \text{ x } 10^{-2}$. The predicted emissivity curves which uses $\epsilon''_{ICE} = 1.73 \text{ x } 10^{-2}$, is also shown.

6.2 Ice Over Rough-Surface SOFI Panel

Figure 15 shows results obtained at 140 GHz for 8.5 mm of ice on the rough-surface SOFI panel. As shown, the h- and v-polarized data is in good agreement with theoretical calculations based on $\epsilon''_i = 5.2 \text{ x } 10^{-2}$. This value is roughly three times larger than what is predicted by Mätzler and Wegmüller [3], whose results at 35 and 94 GHz corresponded so well with ours. Included as well in this figure is a curve representing the *expected* emissivity, generated using the model together with the value of ϵ''_i predicted by extrapolating the results reported by Mätzler and Wegmüller to 140 GHz.. Note that in both cases, the emissivity is dramatically higher than that of the bare SOFI panel, given in Figure 6, illustrating the excellent sensitivity to the presence of ice at 140 GHz.

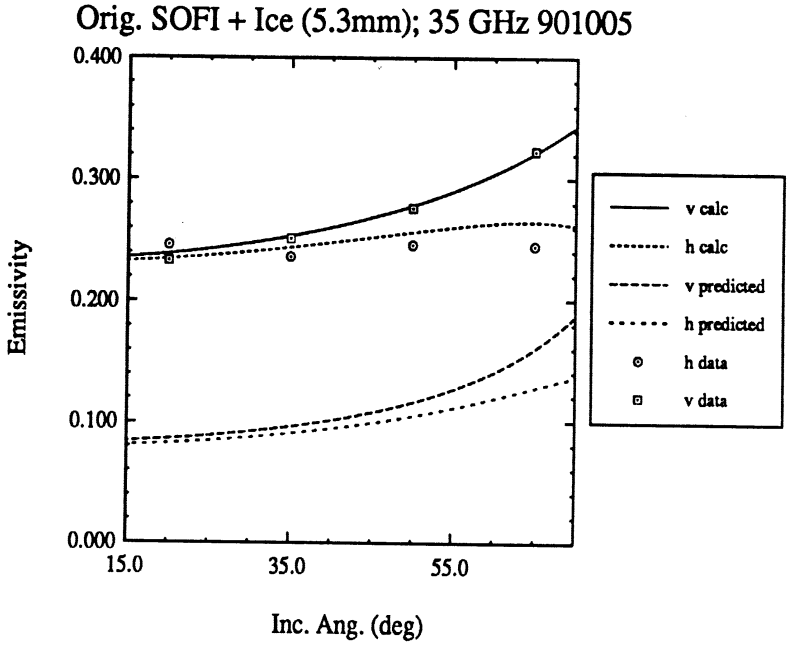

Figure 16: Experimental results obtained at 35 GHz for original rough-surface SOFI panel. The curves which were calculated to fit the data required using ϵ''_{ICE} = 4.77 x 10^{-2}. The predicted emissivity curves which uses ϵ''_{ICE} = 5.6 x 10^{-3}, is also shown.

At 35 GHz, the predicted changes in emissivity as a function of ice thickness are quite small, on the order of 0.01/mm. Figure 16 shows a sample of data taken for an ice layer of 5.3 mm. The magnitude of the emission observed was far larger than what was predicted from the model using experimentally determined dielectric constants. As shown, excellent agreement with calulated values is possible if a value of 4.76 x 10^{-2} is used for ϵ''_i. Subsequent experiments on the ice itself, as described in Section 3, revealed ϵ''_i to be about 8.5 times smaller than the value used to fit the data. The predicted emissivity, obtained using this experimental value of ϵ''_i, is included in the figure for reference.

Observations made of the target with other thicknesses of ice at 35 GHz seemed to give nearly identical results as we had obtained at 5.3 mm. In short, we were unable to obtain significant radiometric sensitivity to ice thickness at 35 GHz.

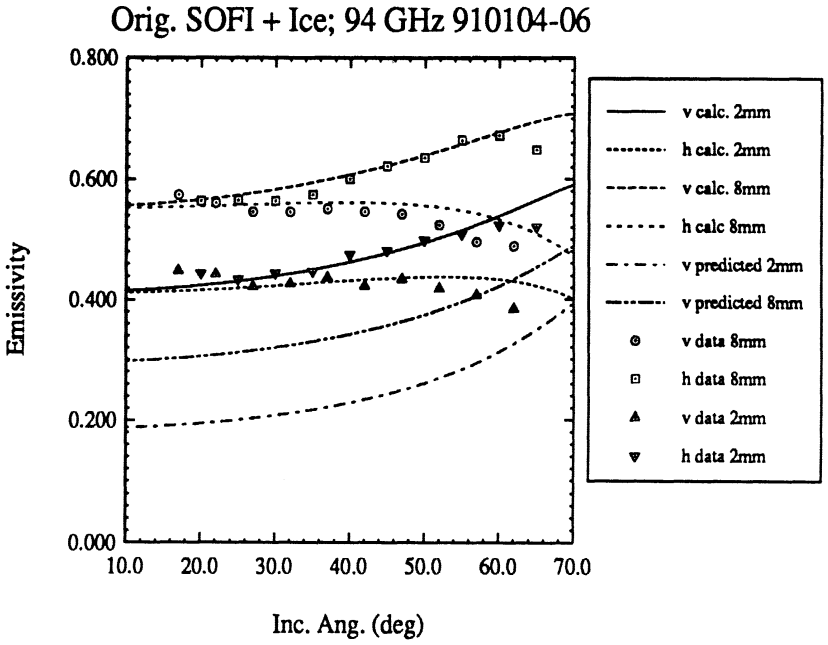

Figure 17: Experimental results obtained at 94 GHz for original rough-surface SOFI panel. The curves which were calculated to fit the data required using ϵ''_{ICE} = 9.0 x 10^{-2} for the 2 mm ice layer, and ϵ''_{ICE} = 4.0 x 10^{-2} for the 8 mm ice layer. The predicted emissivity curves (only v-pol shown) use ϵ''_{ICE} = 1.14 x 10^{-2}.

The results of measurements made of the rough-surface SOFI panel at 94 GHz are shown in Figures 17 and 18. In each figure, the experimental data is shown together with the predicted emissivity. Figure 17 shows the results for two different ice thicknesses which were examined on different days. While these curves show the characteristic behavior for h- and v-polarization, they cannot be simultaneously fit using the same value for ϵ''_i . And the value of ϵ''_i required to fit the data for either ice thickness is much larger than what has been experimentally determined for ice.

Figure 18 represents the results obtained for v-polarization for four different thicknesses of ice. Although the variations with angle and with ice thickness of the experimental data are comparable with those exhibited by the model calculations based on the experimentally determined values of ϵ,

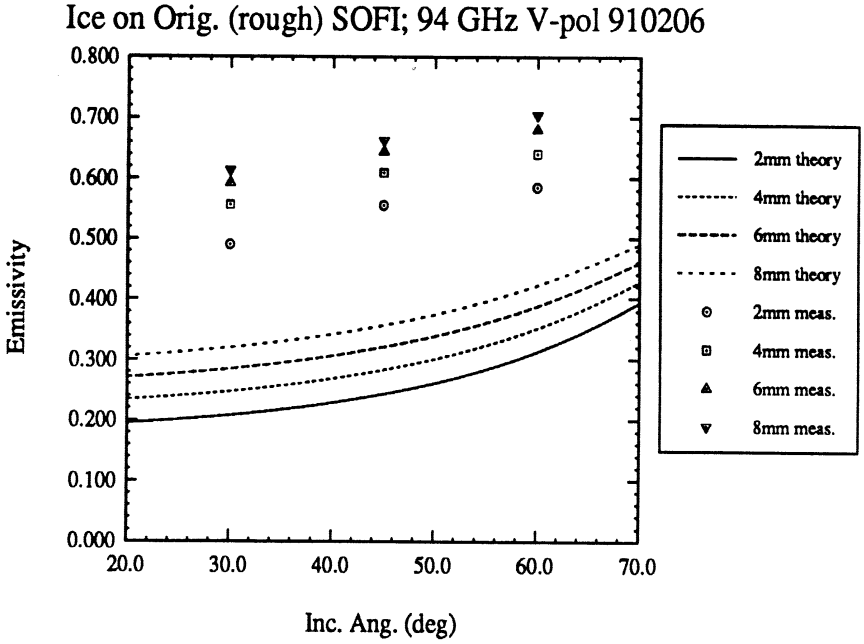

Figure 18: Experimental results for original rough-surface SOFI panel at 94 GHz. Theoretical curves are based on experimentally determined dielectric constants for both the SOFI material and for ice.

the two sets are very different in absolute level. This is attributed to the effects of the rough surface of the SOFI panel.

7 Discussion

7.1 Application to Smooth-Surface SOFI Panel

The results given in the preceding section demonstrate that the behavior of a system of ice over SOFI panel can be quite accurately predicted using an incoherent radiative transfer model, *if* the top surface of the SOFI panel is smooth. For this case, the sensitivity of the method, that is, the change in emissivity with respect to change in ice thickness is illustrated in Figure 19. Here is shown, for a particular incidence angle of 30°, the variation of the emissivity with ice thickness at 35, 94, and 140 GHz for the case of pure ice (Figure 19a) and for the case of frost-like ice, having an ice volume density

v of 0.5 (Figure 19b). Actual data is shown for 94 GHz for the pure ice case; the curves for 35 GHz are based on our experimentally determined value of ϵ_i''; and at 140 GHz we have used a value based on extrapolating the data of Mätzler and Wegmüller [3] for impure ice to 140 GHz. The degree to which our experimental values agree with theirs at 35 and 94 GHz make this a reasonable assumption for 140 GHz.

Figure 20 presents essentially the same information, except that now we show the variation of antenna temperature T_A with ice thickness, which includes the sky reflected contribution (see (1)). In this case, it is necessary to assume a representative value of T_{SKY} for each of the three frequencies. The resulting values for T_A, indicate that for pure ice, the antenna temperature exhibits an approximately linear variation with ice thickness, with a slope of 5.3 K/mm at 140 GHz, 4.1 K/mm at 94 GHz, and 1.1 K/mm at 35 GHz.

7.2 Application to Non-Isothermal Situation

The antenna temperature for a smooth-surface isothermal medium can be expressed as

$$T_A = eT_{PHYS} + (1 - e)T_{SKY}. \tag{19}$$

As alluded to in Section 2, the fueltank/ice system is in reality not an isothermal system. It is more accurately described in terms of a temperature gradient, having a temperature on the order of 94 K at the metal-SOFI interface, and warming to a temperature just below the freezing point of water, about 270 K, at the SOFI-ice interface [2]. For such a temperature profile, the relation

$$R = 1 - e,$$

is no longer completely valid, from conservation of energy principles. In fact, the concept of emissivity cannot legitimately be applied since, by definition,

$$e = \frac{T_B}{T_{PHYS}},$$

and T_{PHYS} is not unique for such a system. Together, these factors make it unclear how the three quantities in (19), T_{AP}, T_{PHYS}, and T_{SKY} can be used to express an intrinsic property of the medium, like emissivity and reflectivity, which can be unambiguously related to structural features of the medium like ice thickness.

The solution to this apparent difficulty lies in the introduction of a quantity, *effective emissivity*, which is defined as,

$$e_{eff} = \frac{T_B}{T_0}, \tag{20}$$

where T_B is the brightness temperature of the non-isothermal medium and T_0 is the temperature of the medium at the surface. (In our case, T_0 is the ice temperature, typically 270 K.) This quantity e_{eff} is not an intrinsic property of the medium—it is dependent on the details of the temperature profile. However, where the temperature profile is relatively well known, e_{eff} may be related to the structural features of the medium. In order to calculate e_{eff} from the three measurable quantities in (19), it is necessary to express the reflectivity R in terms of e_{eff}. We now describe how we obtain such an expresssion.

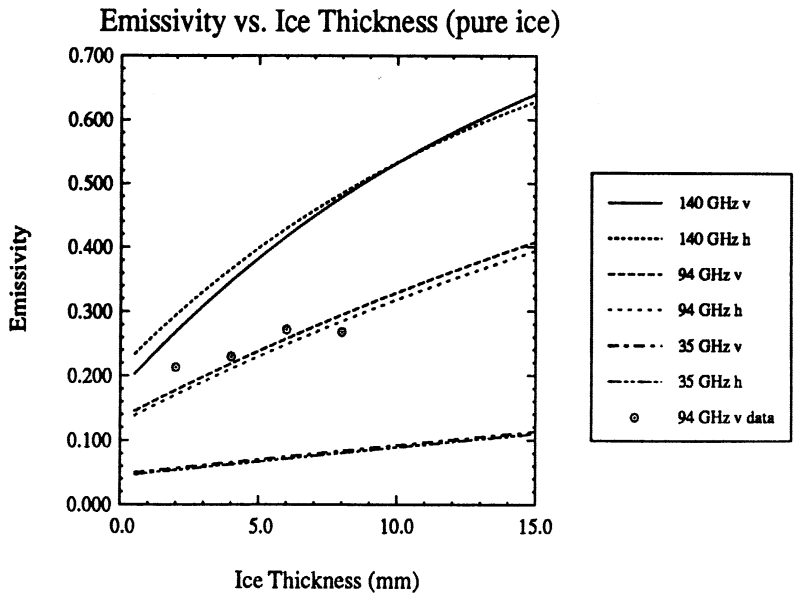

(a)

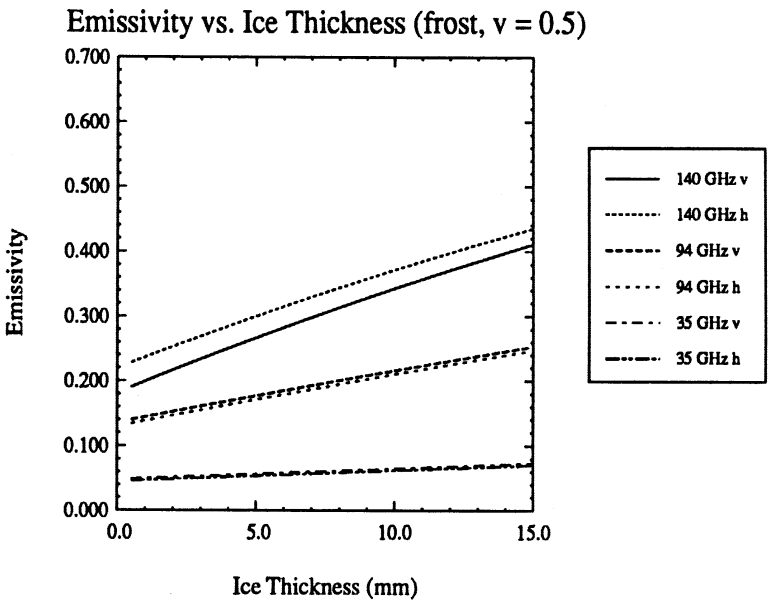

(b)

Figure 19: Isothermal case: Emissivity variation with ice thickness for ice volume density of (a) 1.0 (pure ice) and (b) 0.5 (frost).

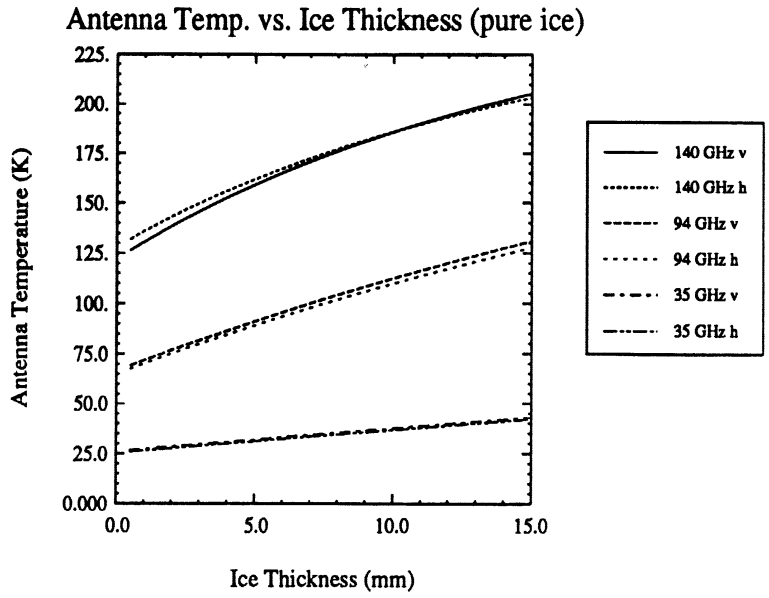

(a)

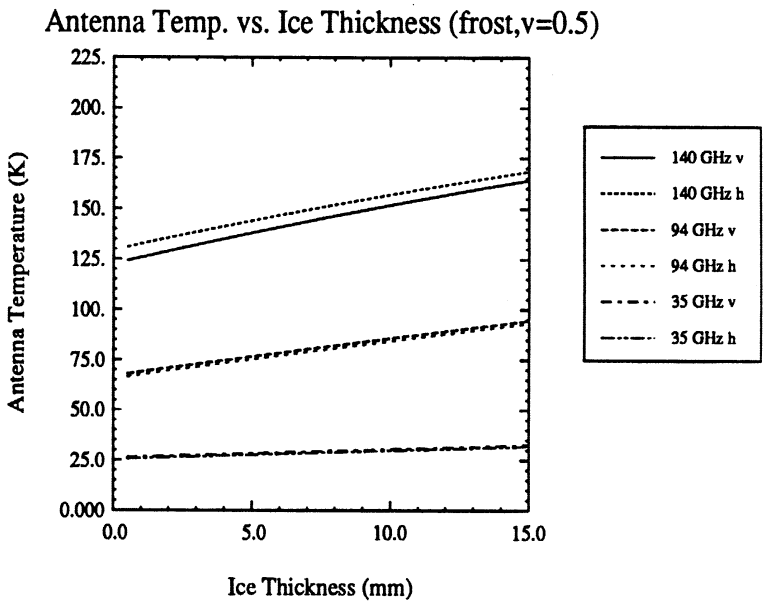

(b)

Figure 20: Antenna temperature variation with ice thickness for ice volume density of (a) 1.0 (pure ice) and (b) 0.5 (frost). Assumes $T_{PHYS} = 270K$ and T_{SKY} = 14, 35, and 90K for 35, 94, and 140 GHz respectively.

7.2.1 Relating R and e_{eff}

The brightness temperature T_B may be computed for a medium having a temperature gradient using the model presented in Appendix B, and then (20) can be applied to find e_{eff}. The reflectivity of this medium is *independently* determined by using the *isothermal* model of Appendix A to compute the emissivity, and then applying the relation $R = 1 - e$. Note that this reflectivity computed for the isothermal case is *equally valid* for the temperature gradient case since it is a property of the material itself, *not* of the temperature profile of the material.

This procedure is repeated for a series of different ice thicknesses, obtaining a value of e_{eff} (from (20)) and of R for each case. The values for e_{eff} are plotted against those of R, and then a simple curve fit is applied which yields an algebraic expression describing e_{eff} in terms of R. This expression is, in general, valid only for the particular frequency, incidence angle, polarization, and ice volume density for which it was computed. We performed this computation for a series of cases, all with incidence angle of 30°, but using combinations of frequency, polarization, and ice volume density. We found that for each case, there is an exact linear relation between R and e_{eff} of the form,

$$R = b - me_{eff}, \tag{21}$$

so that (19) becomes

$$T_A = e_{eff}T_0 + (b - me_{eff})T_{SKY}. \tag{22}$$

A summary of the slopes and intercepts satisfying (21) for a variety of cases is given in Table 3.

Once measurements of the quantities T_{AP},T_o, and T_{SKY} are obtained, we obtain from (22):

$$e_{eff} = \frac{T_A - bT_{SKY}}{T_0 - mT_{SKY}}, \tag{23}$$

and from this value of e_{eff}, structural details, such as ice thickness, are inferred.

7.2.2 Comparison to Isothermal Case

Figure 21 shows the variation of antenna temperature with ice thickness for the SOFI/ice system having a linear temperature gradient. A comparison

	Vertical Polarization				Horizontal Polarization			
	Frost (v=0.5)		Ice (v=1.0)		Frost (v=0.5)		Ice (v=1.0)	
Freq. (GHz)	m	b	m	b	m	b	m	b
35	0.990	0.984	0.993	0.984	0.985	0.985	0.994	0.985
94	0.971	0.953	0.971	0.953	0.974	0.955	0.968	0.956
140	0.962	0.936	0.954	0.935	0.920	0.948	0.938	0.921

Table 3: Values for slope and intercept which relate the reflectivity to the *effective emissivity* for a ice/SOFI system having a linear temperature profile. These values are for the case of a 30° incidence angle.

	Sensitivity (K/mm)	
	Temperature Profile	
Freq. (GHz)	Uniform	Linear
35	1.1	1.1
94	4.1	4.5
140	5.3	5.6

Table 4: Sensitivity, in K/mm, of antenna temperature to changes in ice thickness. Values are for case of 30° incidence angle and pure ice (v = 1.0). Results shown are valid for both polarizations.

of Figure 21 to Figure 20, which treats the isothermal case, reveals that for the temperature gradient case, T_A is somewhat lower, and the sensitivity of antenna temperature to changes in ice thickness is somewhat greater. The latter point is summarized in Table 4 for the pure (v=1.0) ice case.

One implication of these differences is that the accuracy of ice thickness determination is impaired if isothermal-based calculations are used for a system having a temperature gradient. If such an approximation were feasible, the need for determining empirical constants m and b described in this section could be avoided. From Figures 20 and 21, for the pure (v=1.0) ice case, it can be seen that such an attempt would consistently underestimate the ice thickness, by about 2.5 mm for the 94 GHz case, and 1.5-2.0 mm for the 140 GHz case.

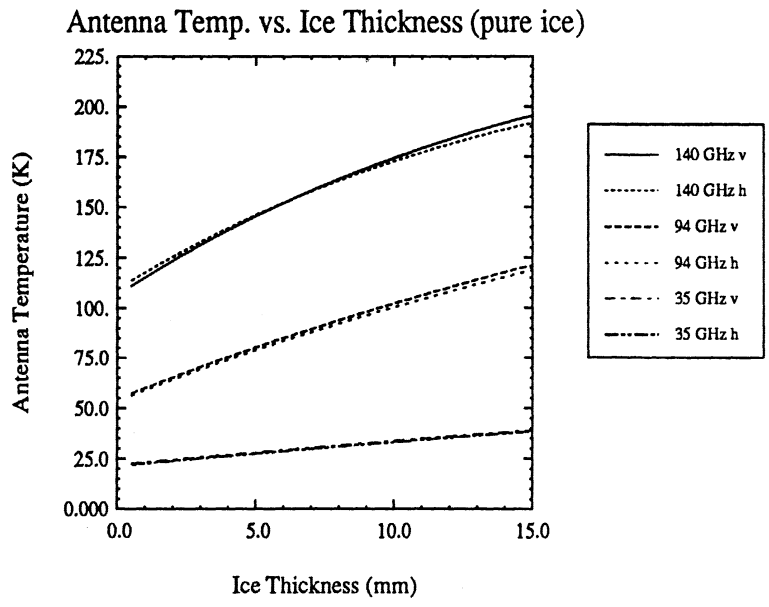

(a)

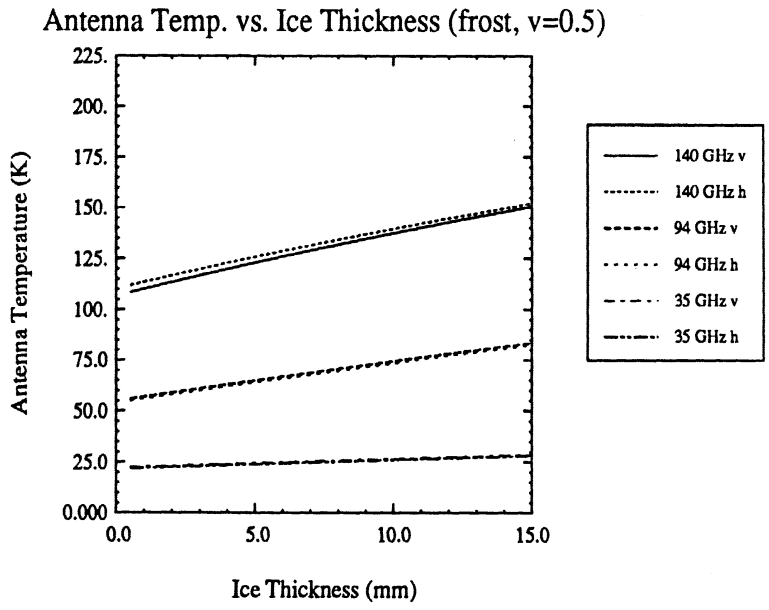

(b)

Figure 21: Temperature gradient case: Antenna Temperature variation with ice thickness for ice volume density of (a) 1.0 (pure ice) and (b) 0.5 (frost). Assumes $T_{PHYS} = 270K$ and $T_{SKY} = 14$, 35, and 90K for 35, 94, and 140 GHz respectively.

7.2.3 Sensitivity to Magnitude of Temperature Gradient

It was shown in the previous section that attempts to estimate ice thickness for a non-isothermal system using isothermal-based computations led to error on the order of 2 mm. One difficulty with the temperature gradient case is that the exact magnitude of the temperature gradient might not be known. While the surface temperature of the ice/SOFI system can be relatively easily determined, there would likely be more uncertainty in knowing the temperature at the metal/SOFI interface. A logical question is how seriously would incorrect descriptions of the temperature gradient affect the accuracy of the ice thickness estimations.

This question is answered in Figure 22, for specific cases of frequency, ice thickness, and ice volume density. For each case, the temperature at the metal/SOFI interface, which is reported to be 94 K [2], is allowed to vary over the range from 50 K to 140 K. As can be seen, the antenna temperature is quite insensitive such variations. In quantitative terms, for the 140 GHz case of 9 mm of pure ice, the value of $\delta T_A/\delta T_M$, where T_M is the temperature at the metal/SOFI interface is just 0.06 K/K. This means that, from the sensitivity cited in Table 4, T_M must be different from 94 K by 80 K to induce an ice thickness estimation error of 1 mm.

8 Conclusion

The purpose of this investigation has been to determine whether it is feasible to sense the presence and thickness of ice on the surface of the Space Shuttle fueltank using a radiometer operating at millimeter wave frequencies. More specifically, we have tried to determine whether intrinsic material quantities such as emissivity and reflectivity, derived from radiometric measurements, could be used to predict ice thickness.

For the case in which the normally rough fueltank material (SOFI) has been made smooth, we have demonstrated that a model based on first order radiative transfer theory can correctly predict emissivity for a given ice thickness. We have verified this model with experiments performed on a system of ice/SOFI in an isothermal state, and have shown how the technique can be extended to the more realistic case of a temperature gradient.

For the case of a system having a temperature gradient, we have demon-

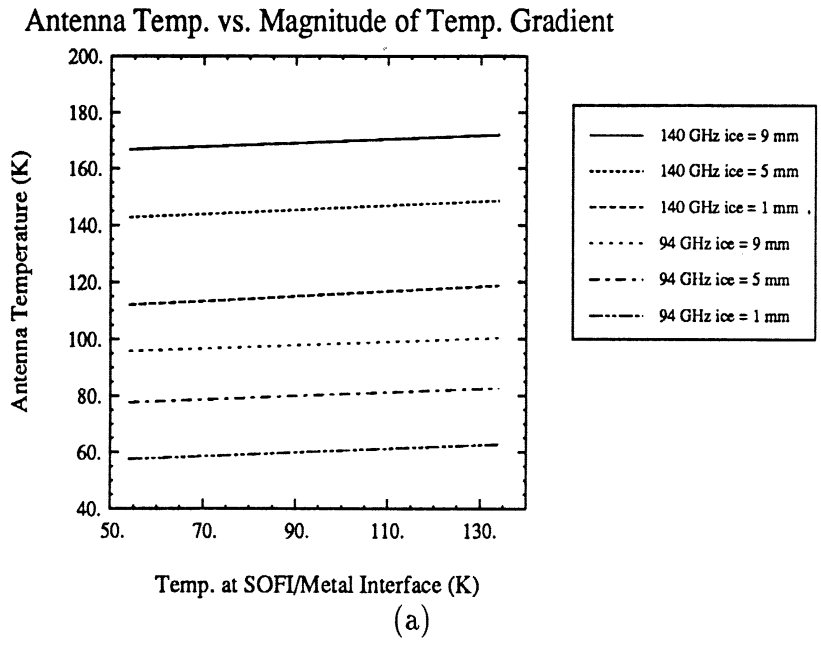

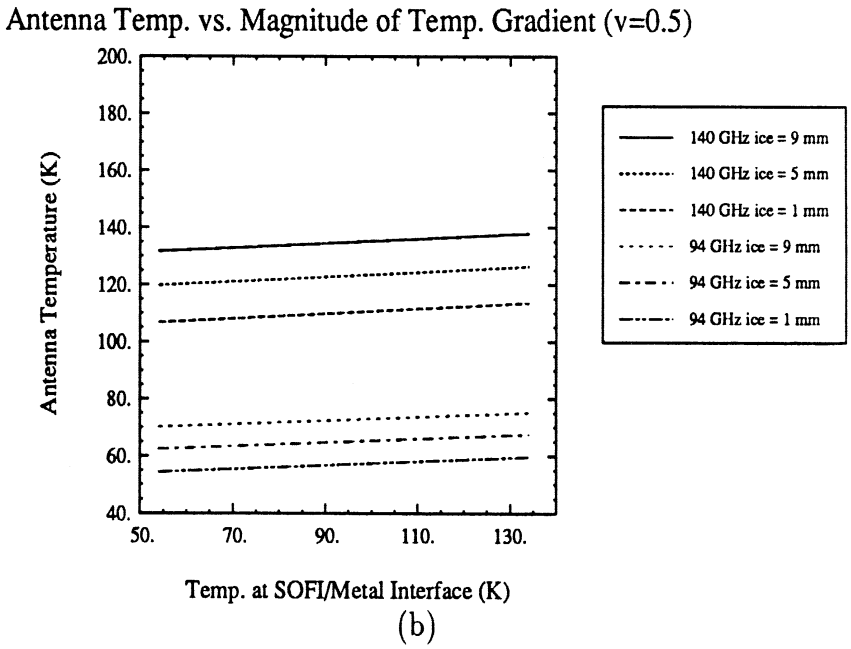

Figure 22: Sensitivity of antenna temperature to magnitude of temperature gradient, computed for cases of (a) pure ice (v=1.0) and (b) frost (v=0.5).

strated that isothermal-based computations cannot be applied without introducing errors, which may be as much as 2.5 mm, in the estimation of ice thickness. We have further shown that when using temperature- gradient-based computations, the critical parameter is the surface temperature (i.e., ice temperature). The temperature at the metal/SOFI interface can be significantly mis-assigned without inducing any serious error in the ice thickness estimation.

For the case of the SOFI material in its original (rough-surface) state, we have observed that the emission is modified significantly beyond what is predicted by the smooth-surface model described above. This case should be the subject of a future investigation.

References

[1] Ulaby,F.T., R.K. Moore, and A.K. Fung, *Microwave Remote Sensing*, vol.3, Artech House, Dedham, Mass., 1986.

[2] Wu, S., NASA Stennis Research Center, personal communication.

[3] Mätzler, C., and U. Wegmüller, "Dielectric Properties of Fresh Water Ice at Microwave Frequencies," *J. Phys. D: Applied Physics*, vol. 20, 1987, pp. 1623-1630.

[4] Ulaby,F.T., R.K. Moore, and A.K. Fung, *Microwave Remote Sensing*, vol.1, Addison-Wesley, Reading, Mass., Ch. 4, 1981.

APPENDIX A: Emission Model For Ice Layer Over SOFI Panel With Uniform Temperature Profile

Figure A.1 shows the geometry of the problem. The radiometer incidence angle is θ_o, the transmission angle is θ_1 in layer 1 (ice) and θ_2 in layer 2 (SOFI material). These angles are given by

$$\theta_1 = \sin^{-1}\left(\sin\theta_o/\sqrt{\epsilon_1'}\right), \tag{A.1}$$

$$\theta_2 = \sin^{-1}\left(\sin\theta_o/\sqrt{\epsilon_2'}\right), \tag{A.2}$$

The ice layer has relative dielectric constant ϵ_1 and extends from $z = 0$ to $z = -d_1$, the SOFI layer has dielectric constant ϵ_2 and extends from $-d_1$ to $-d_2$, and both layers are at the same physical temperature T_0.

In layer 1, we shall use $T_1^+(z)$ to denote the upwelling radiation (Figure A.2) and $T_1^-(z)$ to denote the downwelling radiation. At the air-ice boundary inside layer 1, the upwelling radiation propagating at an angle θ_1 relative to the z axis is given by:

$$T_1^+(0) = T_1^+(-d_1)\Upsilon_1 + T_0(1 - \Upsilon_1) \tag{A.3}$$

where $T_1^+(-d_1)$ is the upwelling radiation inside layer 1 at the ice-SOFI boundary and Υ_1 is the one-way transmissivity of the layer,

$$\Upsilon_1 = \exp(-\kappa_1 d_1 \sec\theta_1) \tag{A.4}$$

with

$$\kappa_1 = \frac{2\pi}{\lambda}\frac{\epsilon_1''}{\sqrt{\epsilon_1'}}. \tag{A.5}$$

The first term in (A.3) represents the radiation at the bottom of the layer ($T_1^+(-d_1)$) multiplied by the transmissivity of the layer, and the second term

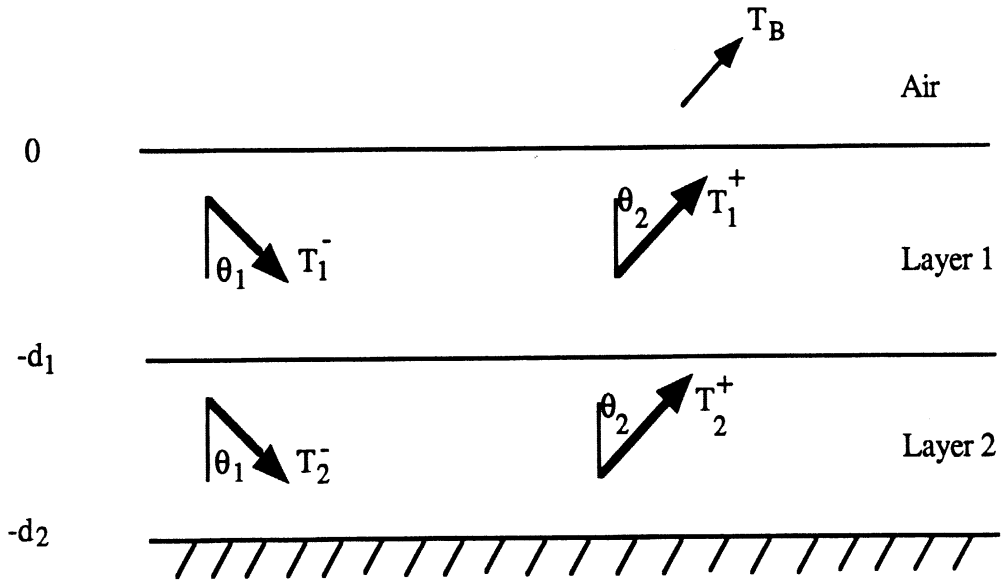

Figure A.1: Geometry of emission for uniform temperature profile case. The quantities T_1^+ and T_2^+ represent upwelling radiation in layers 1 and 2, and T_1^- and T_2^- represent downwelling radiation.

represents the self-emitted radiation generated by the layer. A similar equation can be written for the downward emitted radiation inside layer 1 at the ice-SOFI boundary ($z = -d_1$),

$$T_1^-(-d_1) = T_1^-(0)\Upsilon_1 + T_0(1 - \Upsilon_1), \tag{A.6}$$

and similar expressions apply to layer 2,

$$T_2^+(-d_1) = T_2^+(-d_2)\Upsilon_2 + T_0(1 - \Upsilon_2), \tag{A.7}$$

$$T_2^-(-d_2) = T_2^-(-d_1)\Upsilon_2 + T_0(1 - \Upsilon_2), \tag{A.8}$$

where

$$\Upsilon_2 = \exp[-\kappa_2(d_2 - d_1)\sec\theta_2], \tag{A.9}$$

and

$$\kappa_2 = \frac{2\pi}{\lambda}\frac{\epsilon_2''}{\sqrt{\epsilon_2'}}. \tag{A.10}$$

The boundary conditions at $z = 0$ and $z = -d_1$, inside layer 1, are:

$$T_1^-(0) = R_0 T_1^+(0) \tag{A.11}$$

$$T_1^+(-d_1) = R_1 T_1^-(-d_1) + (1 - R_1) T_2^+(-d_1), \tag{A.12}$$

where R_0 is the ice-to-air Fresnel reflectivity at incidence angle θ_1, which is equal to the air-to-ice reflectivity at incidenve angle θ_0, and similarly, R_1 is the ice-to-SOFI Fresnel reflectivity at θ_1. With $i = 0$ or 1,

$$R_i = \left| \frac{\sqrt{\epsilon_i}\cos\theta_i - \sqrt{\epsilon_{i+1}}\cos\theta_{i+1}}{\sqrt{\epsilon_i}\cos\theta_i + \sqrt{\epsilon_{i+1}}\cos\theta_{i+1}} \right|^2, \textit{for } h \textit{ polarization}, \tag{A.13}$$

$$R_i = \left| \frac{\sqrt{\epsilon_{i+1}}\cos\theta_i - \sqrt{\epsilon_i}\cos\theta_{i+1}}{\sqrt{\epsilon_{i+1}}\cos\theta_i + \sqrt{\epsilon_i}\cos\theta_{i+1}} \right|^2, \textit{for } v \textit{ polarization}. \tag{A.14}$$

The boundary conditions at $z = -d_1$, and $z = -d_2$ inside layer 2 are:

$$T_2^-(-d_1) = R_1 T_2^+(-d_1) + (1 - R_1) T_1^-(-d_1), \tag{A.15}$$

$$T_2^+(-d_2) = T_2^-(-d_2). \tag{A.16}$$

Upon using the boundary conditions (A.11), (A.12), (A.15), and (A.16) in (A.3), (A.6), (A.7) and (A.18), and after some algebraic manipulations, we obtain the following expression for $T_1^+(0)$, the upwelling radiation inside layer 1 at $z = 0$ (just beneath the upper ice surface):

$$T_1^+(0) = \left[\frac{(1 - R_1\Upsilon_2^2) - R_1\Upsilon_1^2(1 - \Upsilon_2^2) - \Upsilon_1^2\Upsilon_2^2(1 - R_1)}{(1 - R_1\Upsilon_2^2)(1 - R_0R_1\Upsilon_1^2) - \Upsilon_1^2\Upsilon_2^2R_0(1 - R_1)^2} \right] T_0 \tag{A.17}$$

The brightness temperature T_B is the upwelling radiation transmitted across the air-ice boundary into the uppermost layer (air),

$$T_B = (1 - R_0)T_1^+(0). \tag{A.18}$$

Since the ice and SOFI layers are at the same temperature T_0, we can define an emissivity e given by

$$e = \frac{T_B}{T_0} \tag{A.19}$$

$$= (1 - R_0)\left[\frac{(1 - R_1\Upsilon_2^2) - R_1\Upsilon_1^2(1 - \Upsilon_2^2) - \Upsilon_1^2\Upsilon_2^2(1 - R_1)}{(1 - R_1\Upsilon_2^2)(1 - R_0R_1\Upsilon_1^2) - \Upsilon_1^2\Upsilon_2^2R_0(1 - R_1)^2}\right]T_0, \tag{A.20}$$

and a corresponding reflectivity R given by

$$R = 1 - e. \tag{A.21}$$

APPENDIX B: Emission Model For Ice Layer Over SOFI Panel With Linear Temperature Profile

This problem is similar to that treated in Appendix A except now the temperature in layer 2 varies linearly from T_1 at $z = -d_2$ to T_0 at $z = -d_1$, as shown in Figure B.1.. Thus,

$$T(z) = \begin{cases} T_0, & \text{for } 0 \leq z \leq -d_1, \\ a + bz, & \text{for } -d_1 \leq z \leq -d_2. \end{cases} \tag{B.1}$$

with

$$a = T_0 + d_1 \frac{(T_0 - T_1)}{d_2 - d_1} \tag{B.2}$$

$$b = \frac{T_0 - T_1}{d_2 - d_1} \tag{B.3}$$

Inside layer 2, the upwelling radiation at $z = 0$, $T_1^+(0)$, and the downwelling radiation at $z = -d_1$, $T_1^-(-d_1)$, are given by (A.3) and (A.6), namely

$$T_1^+(0) = T_1^+(-d_1)\Upsilon_1 + T_0(1 - \Upsilon_1), \tag{B.4}$$

$$T_1^-(-d_1) = T_1^-(0)\Upsilon_1 + T_0(1 - \Upsilon_1). \tag{B.5}$$

Inside layer 2, the upwelling radiation at $z = -d_1$ and the downwelling radiation at $z = -d_2$ are given by:

$$T_2^+(-d_1) = T_2^+(-d_2)\Upsilon_2 + T_{u2}(-d_1), \tag{B.6}$$

$$T_2^-(-d_2) = T_2^-(-d_1\Upsilon_2 + T_{d2}(-d_2), \tag{B.7}$$

where T_{u2} and T_{d2} represent the self-emitted upwelling radiation of layer 2 at $z = -d_1$ and the self-emitted downwelling radiation of layer 2 at $z = -d_2$, and can be computed by evaluating the integral equations

$$T_{u2}(-d_1) = \int_{-d_2}^{-d_1} \kappa_2 \sec\theta_2 T(z) e^{\kappa_2 \sec\theta_2 (z+d_1)} dz \tag{B.8}$$

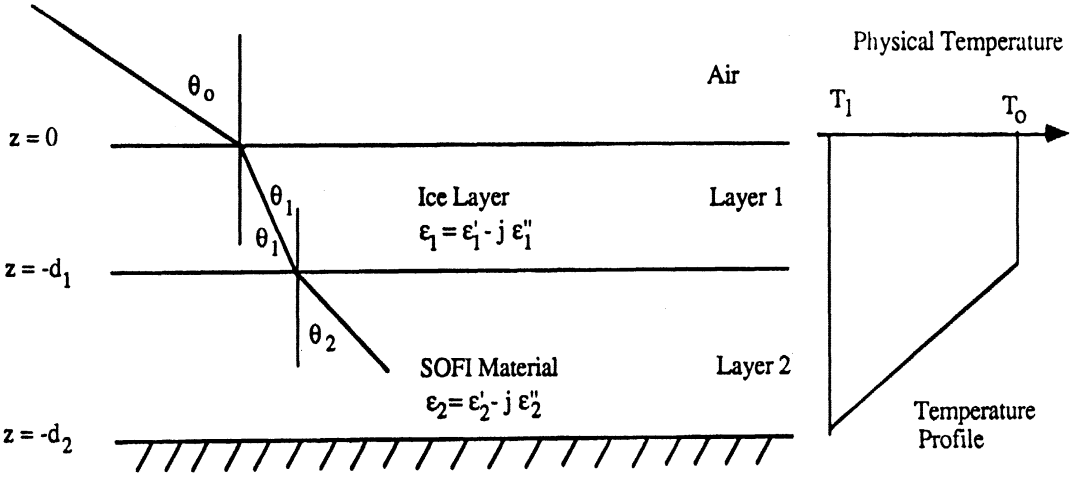

Figure B.1: Geometry of emission for linear temperature profile in layer 2, $T(z) = T_0 + (z + d_1)(T_0 - T_1)/(d_2 - d_1)$for $-d_2 \leq z \leq -d_1$ and a uniform profile in layer 1, $T(z) = T_0$for $-d_1 \leq z \leq 0$.

$$T_{d2}(-d_2) = -\int_{-d_1}^{-d_2} \kappa_2 \sec\theta_2 T(z) e^{-\kappa_2 \sec\theta_2 (d_2+z)} dz. \tag{B.9}$$

Inserting $T(z)$ from (B.1) in (B.8) and (B.9) and integrating, we obtain the results:

$$T_{u2}(-d_1) = T_1(1 - \Upsilon_2) + \delta \tag{B.10}$$

$$T_{d2}(-d_2) = T_0(1 - \Upsilon_2) - \delta \tag{B.11}$$

where

$$\delta = \frac{(T_0 - T_1)}{\tau_s}[(\tau_s - 1) + \Upsilon_2] \tag{B.12}$$

$$\tau_s = \kappa_2 \sec\theta_2 (d_2 - d_1). \tag{B.13}$$

Upon using the boundary conditions given by (A.11), (A.12), (A.15), and (A.16) together with (B.4) - (B.7), we obtain the following expression for $T_1^+(0)$:

$$
\begin{aligned}
T_1^+(0) &= \{\, T_0\,[(1-\Upsilon_1)[(1+\Upsilon_1 R_1)(1-\Upsilon_2^2 R_1)+\Upsilon_1\Upsilon_2^2(1-R_1)^2] \\
&+ \Upsilon_1\Upsilon_2(1-\Upsilon_2)(1-R_1)\,] + T_1\Upsilon_1(1-R_1)(1-\Upsilon_2) \\
&+ \delta[\Upsilon_1(1-R_1)-\Upsilon_1\Upsilon_2(1-R_1)]\,\}\,\mathrm{x}[(1-\Upsilon_2^2 R_1)(1-\Upsilon_1^2 R_0 R_1) \\
&- \Upsilon_1^2\Upsilon_2^2 R_0(1-R_1)^2]^{-1},
\end{aligned}
$$

and the brightness temperature is given by

$$T_B = (1-R_0)T_1^+(0). \tag{B.14}$$

C "Radcal6" Program Listing

This appendix contains the computer program utilized in the experimental portion of our investigation. The program, written in QuickBasic©, was used in conjunction with a Stanford Model SR510 Lock-in Amplifier. This system was then used to control the settings of the amplifier, aquire and store data, and compute and display antenna temperature.

```
'*************************************************************************
'
' Radcal6:
' Program to compute radiometric temperatures.  Calibration is done
' using an ambient ("hot") load and a liquid nitrogen ("cold") load.
' This program is configured to read voltage values from a Stanford
' Instruments (model SR510) lock-in amplifier, upon command. Using
' the calibration equation which this program produces, temperatures
' are returned as output for voltage value input.  These temperatures,
' along with calculated uncertainties, are stored in a file, whose name
' is the current date and with extension "m"; ie. yymmdd.m; eg. 910128.m.
' There is also a calibration file stored for each day, yymmdd.c.
'
'   Additionally, the program allows for background subtraction for
' cases where the target is not beam-filling.
'
'          Written by:  John R. Kendra
'                       University of Michigan
'                       June, 1990
'       Latest Revision: Jan. 22, 1991  (added comments)
'
'*************************************************************************

DECLARE SUB tbgnd (tag%, tb!(), bgnd!(), eta!())
DECLARE SUB dielectric (today$)
DECLARE SUB stat (v!(), xbar!, sd!)
DECLARE SUB calpoints (f!, tmp$, xbar!, hbar!(), cbar!())
DECLARE SUB tbright (f!, m!(), b!(), v(), tb())
DECLARE SUB compute (tamb!, cbar!(), hbar!(), m!(), b!(), bgnd())
DECLARE SUB Calibrate (today$, m(), b(), bgnd())
DECLARE SUB Measure (today$, m(), b())
DECLARE SUB readin (v!())


OPTION BASE 1

'*********************************
```

```
'Establish connection to SR510, initialize settings.

'*********************************

OPEN "com1:9600,N,8,2,cs,ds,cd" FOR RANDOM AS #2
PRINT #2, "I1"
PRINT #2, "B1"
PRINT #2, "C1"
PRINT #2, "D0"
PRINT #2, "E0"
PRINT #2, "G15"
PRINT #2, "L1,1"
PRINT #2, "L2,1"
PRINT #2, "M0"
PRINT #2, "O0"
PRINT #2, "P0"
PRINT #2, "R0"
PRINT #2, "S0"
PRINT #2, "T1,7"
PRINT #2, "T2,2"

'*********************************

'Dimension Main Arrays:
'       m()   = Calibration curve slopes for 35,94,& 140 GHz.
'       b()   = Calibration curve intercepts for 35,94, & 140 GHz.
'       v()   = Four voltage values read in from SR510.
'       tb()  = Four brightness temps. computed corresponding to voltages.
'       eta() = Mainlobe efficiencies for each freq. and polarization.
'       bgnd()= Background correction parameter unique to each freq.
'  and pol.

'************************************

DIM m(3), b(3), v(4), tb(4), eta(6), bgnd(6)

'************************************

'Initialize Main Lobe Efficiencies.

'************************************

eta(1) = .948       'f=35,p=h
eta(2) = .945       'f=35,p=v
eta(3) = .929       'f=94,p=h
eta(4) = .945       'f=94,p=v
eta(5) = .875       'f=140,p=h
eta(6) = .835       'f=140,p=v

'************************************

'Initialize bgnd values:

'************************************
```

```
bgnd(1) = 0
bgnd(2) = 0
bgnd(3) = 0
bgnd(4) = 0
bgnd(5) = 0
bgnd(6) = 0
CLS
LINE INPUT "input today's date (yymmdd):", today$

'****************************************

' Begin main program loop.

'****************************************

DO
    INPUT "Calibrate, measure, compute diel. const.,or
 quit (c,m,d,q) :", char$
    SELECT CASE char$
        CASE "q"
            END
        CASE "c"
            CALL Calibrate(today$, m(), b(), bgnd())
        CASE "m"
            title$ = today$ + ".m"
            OPEN title$ FOR APPEND AS #1
            flag = 0!

'****************************************

'Setup main screen for "Measure" environment.

'****************************************

            CLS
            LOCATE 22, 1
            PRINT "F1 = Target"
            LOCATE 22, 20
            PRINT "F2 = IncAng"
            LOCATE 22, 40
            PRINT "F3 = Polarize."
            LOCATE 22, 60
            PRINT "F4 = Cal_Restore"
            LOCATE 23, 1
            PRINT "F5 = Freq."
            LOCATE 23, 20
            PRINT "F6 = TakeData"
            LOCATE 23, 40
            PRINT "F7 = Quit"
            LOCATE 23, 60
            PRINT "F8 = Background"
            divide$ = STRING$(60, "*")
            LOCATE 21, 5
            PRINT divide$
```

```
            VIEW PRINT 7 TO 20
            target$ = "sky"
            f = 35
            PRINT #2, "G13"
            pol$ = "h"
            ang = 45

'*******************************

'Initialize header of "Measure" environment with defaults.  Procedure
'"Header" does this.  It is called every time one of the parameters is
'altered.

'*******************************

            GOSUB header
        DO

'*******************************

'Initialize softkeys in "Measure" environment.

'*******************************

            ON KEY(1) GOSUB target
            ON KEY(2) GOSUB IncAng
            ON KEY(3) GOSUB Polarize.
            ON KEY(4) GOSUB Calrestore
            ON KEY(5) GOSUB Freq
            ON KEY(6) GOSUB takedata
            ON KEY(7) GOSUB Quit
            ON KEY(8) GOSUB backgnd
            KEY(1) ON
            KEY(2) ON
            KEY(3) ON
            KEY(4) ON
            KEY(5) ON
            KEY(6) ON
            KEY(7) ON
            KEY(8) ON
            LOOP UNTIL flag = 1!
            VIEW PRINT 1 TO 25
            CLS
        CASE "d"
            CALL dielectric(today$)
        CASE ELSE
            PRINT "Selection must be c,m,d, or q"
        END SELECT

'*****************************

'End of main loop of program.

'*****************************
```

```
LOOP

'*********************************************

'Below follows subroutines used only in "Measure" environment.

'*********************************************

target:
LINE INPUT "Enter Target Description:"; target$
GOSUB header
RETURN

IncAng:
INPUT "Enter incidence angle (degrees):", ang
GOSUB header
RETURN

Polarize.:
INPUT "Enter polarization (v/h):", pol$
GOSUB header
RETURN

Calrestore:

'************************************

'This subroutine "Calrestore" reinitializes calibration and background
'variables with their most recent values.  These values are always
' stored
'in a file "junkcal" and this file is read by the "Calrestore" procedure.
'Used when re-entering program after having exited (or crashed!).

'************************************

OPEN "junkcal" FOR INPUT AS #3
FOR i% = 1 TO 3
    INPUT #3, m(i%), b(i%)
NEXT i%
INPUT #3, bgnd(1), bgnd(2), bgnd(3), bgnd(4), bgnd(5), bgnd(6)
PRINT "Most recent calibration parameters restored."
CLOSE #3
RETURN

Freq:
INPUT "Enter Frequency (GHz):", f

'*****************************************

'Gain and phase of SR510 are set for each separate frequency.

'*****************************************

IF f = 35 THEN
        PRINT #2, "G13"
```

```
        PRINT #2, "PO"
ELSEIF f = 94 THEN
        PRINT #2, "G15"
        PRINT #2, "PO"
ELSEIF f = 140 THEN
        PRINT #2, "G12"
        PRINT #2, "P 180.0"
ELSE
END IF
GOSUB header
RETURN

takedata:
    CALL readin(v())
    INPUT "Compute temp. with background adjustment? (If computing
 background, choose 'n'.) (y/n)", p$
    IF p$ = "n" THEN
        CALL tbright(f, m(), b(), v(), tb())
    ELSE
        CALL tbright(f, m(), b(), v(), tb())
        CALL tbgnd(tag%, tb(), bgnd(), eta())
    END IF
    CALL stat(tb(), xbar, sd)
    PRINT "For f =  "; f; "GHz"; "  T-apparent =  "; xbar; "+/- "; sd
    INPUT "Save Data? (y/n):", pp$
    SELECT CASE pp$
        CASE "y"
    WRITE #1, target$, DATE$, "pol. = ", pol$, "inc. ang. = ", ang
    WRITE #1, f, v(1), v(2), v(3), v(4), "Ta = ", xbar, "+/-", sd, TIME$
    WRITE #1, divide$
        CASE ELSE
    END SELECT
RETURN

Quit:
flag = 1!
CLOSE #1
RETURN

header:
place = CSRLIN
VIEW PRINT 2 TO 2
blankout$ = SPACE$(70)
LOCATE 2, 5
PRINT blankout$,
LOCATE 2, 5
PRINT "Description:  "; target$;
VIEW PRINT 4 TO 4
LOCATE 4, 5
PRINT USING "Freq. = ### GHz"; f;
LOCATE 4, 25
PRINT "Pol. = "; pol$;
LOCATE 4, 38
PRINT USING "Inc. Ang. = ###.#"; ang;
VIEW PRINT 5 TO 5
```

```
LOCATE 5, 5
PRINT divide$;
VIEW PRINT 7 TO 20
LOCATE place, 1
SELECT CASE f
CASE 35
        IF pol$ = "h" THEN
                tag% = 1
        ELSE
                tag% = 2
        END IF
CASE 94
        IF pol$ = "h" THEN
                tag% = 3
        ELSE
                tag% = 4
        END IF
CASE ELSE
        IF pol$ = "h" THEN
                tag% = 5
        ELSE
                tag% = 6
        END IF
END SELECT
RETURN

clscreen:
CLS 2
RETURN

backgnd:
INPUT "For background correction, next target must be absorber.
  Continue (y/n):", p$
IF p$ <> "y" THEN
        PRINT "Background evaluation procedure exited."
        RETURN
END IF
INPUT "Enter Temp. (C) of Absorber:", Tabs
Tabs = Tabs + 273
INPUT "Ready to take data (y/n):", p$
IF p$ <> "y" THEN RETURN
GOSUB takedata
bgnd(tag%) = xbar - eta(tag%) * Tabs
Tsl = bgnd(tag%) / (1 - eta(tag%))
PRINT USING "T-side lobe = ###.# K"; Tsl
PRINT "Calculated Background parameters stored."
OPEN "junkcal" FOR OUTPUT AS #3
FOR i% = 1 TO 3
        WRITE #3, m(i%), b(i%)
NEXT i%
WRITE #3, bgnd(1), bgnd(2), bgnd(3), bgnd(4), bgnd(5), bgnd(6)
CLOSE #3
RETURN
```

```
CLOSE #2
STOP
END

SUB Calibrate (today$, m(), b(), bgnd()) STATIC
DIM cbar(3), hbar(3), v(4)
PRINT "Currently in calibration procedure"
title$ = today$ + ".c"
OPEN title$ FOR APPEND AS #1
WRITE #1, "cal. file", DATE$
DO
    INPUT "Enter hot or cold or quit (h,c,or q):", tmp$
    SELECT CASE tmp$
        CASE "h"
            INPUT "Enter ambient temperature (C):", tamb
            tamb = tamb + 273
            WRITE #1, "hot load"
        CASE "c"
            WRITE #1, "cold load"
        CASE "q"
            INPUT "Want to compute slope and intercept? (y,n):", answ$
            IF answ$ = "y" THEN
            CALL compute(tamb, cbar(), hbar(), m(), b(), bgnd())
            WRITE #1, "slopes for 35,94,and 140 GHz are:",
m(1), m(2), m(3)
            WRITE #1, "intercepts are
b(1), b(2), b(3)
            PRINT "slopes for 35,94 and 140 Ghz are:",
m(1), m(2), m(3)
            PRINT "intercepts are
b(1), b(2), b(3)
            EXIT DO
            ELSE
            EXIT DO
            END IF
        CASE ELSE
            PRINT "Must enter h,c, or q."
    END SELECT
DO
    INPUT "Enter current frequency (GHz) (0 to quit):", f
    IF f = 35 THEN
        PRINT #2, "G13"
        PRINT #2, "P0"
    ELSEIF f = 94 THEN
        PRINT #2, "G15"
        PRINT #2, "P0"
    ELSEIF f = 140 THEN
        PRINT #2, "G12"
        PRINT #2, "P180"
    ELSE
    END IF
    SELECT CASE f
        CASE IS > 0
        DO
                INPUT "take data? (y/n):", p$
```

```
            IF p$ = "y" THEN
          CALL readin(v())
          CALL stat(v(), xbar, sd)
          CALL calpoints(f, tmp$, xbar, hbar(), cbar())
          WRITE #1, f, v(1), v(2), v(3), v(4), xbar, sd, TIME$
          PRINT "for f = ", f, "  xbar = ", xbar, " sd = ", sd
          EXIT DO
          ELSE
            EXIT DO
          END IF
          LOOP
        CASE IS <= 0
          EXIT DO
    END SELECT
  LOOP
LOOP
WRITE #1, STRING$(20, "***")
CLOSE #1
END SUB

SUB calpoints (f, tmp$, xbar, hbar(), cbar()) STATIC
IF tmp$ = "c" THEN
    IF f = 35 THEN
        cbar(1) = xbar
    ELSEIF f = 94 THEN
        cbar(2) = xbar
    ELSE
        cbar(3) = xbar
    END IF
ELSE
    IF f = 35 THEN
        hbar(1) = xbar
    ELSEIF f = 94 THEN
        hbar(2) = xbar
    ELSE
        hbar(3) = xbar
    END IF
END IF

END SUB

SUB compute (tamb, cbar(), hbar(), m(), b(), bgnd()) STATIC
OPEN "junkcal" FOR OUTPUT AS #3
FOR i% = 1 TO 3
  IF hbar(i%) = 0 THEN
    hbar(i%) = tamb - 80 + cbar(i%)
  END IF
    m(i%) = (tamb - 80) / (hbar(i%) - cbar(i%))
    b(i%) = 80 - m(i%) * cbar(i%)
    WRITE #3, m(i%), b(i%)
NEXT i%
WRITE #3, bgnd(1), bgnd(2), bgnd(3), bgnd(4), bgnd(5), bgnd(6)
CLOSE #3
END SUB
```

```
SUB dielectric (today$)

'************************************************************************
' This subroutine can calculate dielectric constants (real part only)
' for the special case of an infinite halfspace having a loss tangent
' << 1.

' INPUTS:   - Apparent (measured) temperature,
'           - Physical temperature of halfspace,
'           - Sky temperature, Incidence Angle, Polarization.
' OUTPUTS:  Emissivity, Dielectric constants (there are two roots; pick
'           the reasonable one.)
'************************************************************************

title$ = today$ + ".m"
OPEN title$ FOR APPEND AS #1
divide$ = STRING$(60, "*")
WRITE #1, divide$
WRITE #1, "Dielectric Computations"

PRINT "Currently in dielectric computation procedure"
DO
INPUT "Input T-ap, T-phys, and T-sky (K):", Tap, Tphys, Tsky
WRITE #1, "T-ap = ", Tap, ",  T-phys = ", Tphys, ",  T-sky = ", Tsky

e = (Tap - Tsky) / (Tphys - Tsky)
WRITE #1, "Emissivity = ", e
PRINT USING "Emissivity = #.####^^^^"; e
e1 = SQR(1 - e)
f0 = (1 + e1) / (1 - e1)
f1 = (1 - e1) / (1 + e1)
DO
INPUT "Enter incidence angle (deg) and polarization (v/h or '0,q' to quit):", ang, p$
WRITE #1, "Inc. Ang. = ", ang, ", and polarization = ", p$
pi = 4 * ATN(1!)
ang = ang * pi / 180!

SELECT CASE p$
    CASE "h"
        eps = (COS(ang)) ^ 2 * f0 ^ 2 + (SIN(ang)) ^ 2
        PRINT "Dielectic constant = "; eps
        WRITE #1, "Dielectric constant =  ", eps
    CASE "v"
        IF f0 ^ 4 >= (SIN(2 * ang)) ^ 2 * f0 ^ 2 THEN
            f = f0
        ELSE
            f = f1
        END IF

        a1 = SQR(f ^ 4 - (SIN(2 * ang)) ^ 2 * f ^ 2)
 / (2 * (COS(ang)) ^ 2)
        a2 = f ^ 2 / (2 * (COS(ang)) ^ 2)
        eps1 = a2 + a1
        eps2 = a2 - a1
        PRINT "Values obtained for dielectric constant are:", eps1, eps2
```

```
        WRITE #1, "Values obtained for dielectric constant are:  ",
 eps1, eps2
    CASE "q"
        EXIT DO
    CASE ELSE
        PRINT "Entry must be 'v','h', or 'q'."
END SELECT
LOOP
INPUT "Do another dielectric computation? (y/n)", p$
IF p$ = "n" THEN EXIT DO
LOOP
WRITE #1, divide$
CLOSE #1
END SUB

SUB readin (v()) STATIC

FOR i% = 1 TO 4
        PRINT #2, "Q"
        INPUT #2, v(i%)
        v(i%) = v(i%) * 1000000!
        PRINT v(i%)
        SLEEP (1)
NEXT i%

END SUB

SUB stat (v(), xbar, sd)
squares = 0
xes = 0
FOR i% = 1 TO 4
    xes = xes + v(i%)
    squares = squares + v(i%) ^ 2
NEXT i%
sd = SQR(squares / 4 - (xes / 4) ^ 2) / SQR(4)
xbar = xes / 4

END SUB

SUB tbgnd (tag%, tb(), bgnd(), eta())
FOR i% = 1 TO 4
        tb(i%) = (tb(i%) - bgnd(tag%)) / eta(tag%)
NEXT i%
END SUB

SUB tbright (f, m(), b(), v(), tb()) STATIC
IF f = 35 THEN
  FOR i% = 1 TO 4
    tb(i%) = m(1) * v(i%) + b(1)
  NEXT i%
ELSEIF f = 94 THEN
  FOR i% = 1 TO 4
  tb(i%) = m(2) * v(i%) + b(2)
  NEXT i%
ELSE
```

```
  FOR i% = 1 TO 4
    tb(i%) = m(3) * v(i%) + b(3)
  NEXT i%
  END IF
END SUB
```

UNIVERSITY OF MICHIGAN
3 9015 02527 8030